Journal of Hydrology 420–421 (2012) 228–244

Contents lists available at SciVerse ScienceDirect

Journal of Hydrology

journal homepage: www.elsevier.com/locate/jhydrol

Trend and magnitude of changes in climate variables and reference evapotranspiration over 116-yr period in the Platte River Basin, central Nebraska–USA

Suat Irmak *, Isa Kabenge, Kari E. Skaggs, Denis Mutiibwa

University of Nebraska-Lincoln, Department of Biological Systems Engineering, 241 L.W. Chase Hall, Lincoln, NE 68583, United States

ARTICLE INFO

Article history:
Received 14 February 2011
Received in revised form 19 October 2011
Accepted 2 December 2011
Available online 13 December 2011
This manuscript was handled by Laurent Charlet, Editor-in-Chief, with the assistance of Martin Beniston, Associate Editor

Keywords:
Climate change
Evapotranspiration
Meteorological variables

SUMMARY

Some studies that investigate the climate change and hydrologic balance relationships utilize reference (potential) evapotranspiration (ET_{ref}) to either calculate the changes in trends and magnitude of actual *ET* or to determine changes in atmospheric demand. In such cases, it is important to acquire robust ET_{ref} estimates to correctly assess the impact of changes in meteorological variables on atmospheric evaporative demand, hydrologic balances, response of vegetation to climate, and their interactions. Despite its crucial importance, unfortunately, ET_{ref} is sometimes poorly addressed in climate change studies as some studies utilize temperature or radiation-based empirical equations due to various reasons (unavailability of climate data to solve combination-based energy balance equations, etc.). Since many climate variables that affect ET_{ref} rates have been changing and are expected to change in the future, single-variable equations for estimating the trend in ET_{ref} should be avoided due to the inherent nature of the trend passed to ET_{ref} from the variable. Here, we showed an integrated approach of practical and robust procedures that are already exist to estimate necessary climate variables [incoming shortwave radiation (R_s), net radiation (R_n), wind speed at 2-m (u_2), relative humidity (RH), and vapor pressure deficit (VPD)] only from observed maximum and minimum air temperatures (T_{max} and T_{min}) and precipitation (*P*) data to be used in Penman–Monteith-type combination-based energy balance equations to predict grass-and alfalfa-reference evapotranspiration (ET_o and ET_r, respectively). We analyzed the trends and magnitudes of change in meteorological variables for a 116-yr period from 1893 to 2008 in the agro-ecosystem-dominated Platte River Basin in central Nebraska, USA. Although we found a significant ($P < 0.05$) increase in T_{min} and T_{avg} at a rate 0.038 °C yr^{-1} and 0.0187 °C yr^{-1}, respectively, and insignificant increase in u_2 and VPD, we observed a significant ($P < 0.05$) decline in ET_{ref} (-0.3596 mm yr^{-1} for ET_o and -0.3586 mm yr^{-1} for ET_r). We present data, analyses, and interpretation that the decrease in ET_{ref} is most likely due to significant ($P < 0.05$) increase in precipitation (0.87 mm yr^{-1}) that results in significant reduction in R_s (-0.0223 MJ m^{-2} yr^{-1}) and, in turn in R_n (-0.0032 MJ m^{-2} yr^{-1}), which resulted in reduction in ET_{ref} because increase in P decreases available energy, which is primary driver of ET_{ref}. There was approximately 100 mm of increase in precipitation from 1893 to 2008 in the study location at a rate of about 0.90 mm yr^{-1}. Also, there was a significant increase in maximum daily precipitation, especially in the very high events (i.e., >70 mm d^{-1}). We present detailed analyses of relationships between ET_{ref} and all meteorological variables. On an annual time step ET_{ref} significantly ($P < 0.05$) and inversely correlated to precipitation and RH, and significantly and positively correlated to T_{max}, T_{avg}, VPD, R_s, and R_n. We observed a higher degree of responsiveness of ET_o to changes in meteorological variables than ET_r, which may indicate that ET_o may be more apposite to better detect the impact of changes in meteorological variables on ET_{ref} in climate change studies.

1. Introduction

The long-term trends and magnitude of changes in climate and environmental parameters such as air temperature, solar and net radiation, cloud cover and precipitation, CO_2 concentration, and their potential consequences that impact the behavior and functioning of agro-ecosystems are crucial variables. Changes in climate variables interact with and impact agro-ecosystem productivity and land surface-atmosphere interactions through various direct and indirect processes. Direct processes include increased air temperature and/or CO_2 concentration, storm surges that cause changes in hydrologic parameters such as precipitation, run-off and stream flow while indirect processes include changing the intensity and frequency of disturbances of wild fires, pests and diseases (IPCC, 2007). The varying magnitude of global temperature

* Corresponding author. Tel.: +1 402 472 4865.
E-mail address: sirmak2@unl.edu (S. Irmak).

0022-1694/$ - see front matter © 2011 Elsevier B.V. All rights reserved.
doi:10.1016/j.jhydrol.2011.12.006

increase has been well-documented by many scientists. The IPCC (1996) reported warming of the earth's atmosphere by between about 0.3 and 0.6 °C since the late 19th century. The global mean land-surface-air temperature has risen by about 0.74 °C over the past 100 yr (1906–2005) and is predicted to increase by 1.1–6.4 °C by 2100 (IPCC, 2007). Houghton et al. (2001) reported a mean annual temperature increase of 1.4–5.8 °C during 20th century. With the increase in temperature, other climatic variables that have strong direct and/or implicit links to temperature such as vapor pressure deficit, incoming shortwave radiation, evaporation from the surface and transpiration from vegetation surfaces, and evapotranspiration (*ET*) from coupled plant/soil interface can be significantly affected. On a large scale, many other climatic variables such as precipitation, wind speed and direction, and relative humidity are also directly or indirectly impacted by changes in atmospheric temperature due to its effect on atmospheric circulation. Among all these variables, perhaps one of the most important ones is the *ET*, which can be the largest component of the hydrologic cycle. Since *ET* is directly linked to these climatic variables, any changes in the variables in conjunction with warmer air temperatures are expected to influence the trends and magnitudes of *ET*.

Studies that investigate changes in climate variables have yielded a mixture of results and conclusions about the trends of climatic variables, especially *ET*, for specific locations. For Pisa Italy, Moonen et al. (2002) found that over a 122-yr period there was a decreasing minimum temperature, decreasing maximum temperature, decreasing precipitation, and decreasing *ET* trend. The *ET* volumes were calculated using the method of Hargreaves and Samani (1982), which is a temperature-based empirical equation. In India, Chattopadhyay and Hulme (1997) calculated *ET* using the Penman method and revealed a decreasing trend over a period of 15 yr (1976–1990) while temperature showed an increasing trend over 50 yr (1940–1990). In the USA, Grundstein (2009) used a modified form of Thornthwaite's moisture index to evaluate climate change. Results reveal statistically significant trends, both positive and negative, for moisture index, temperature and precipitation for geographically cohesive clusters. Zhang et al. (2007) showed a significant decrease in *ET* and pan evaporation for 47 (38%) of the weather station locations they studied, though they observed significant increase in temperature, and decrease in wind speed and sunshine hours on the Tibetan Plateau. Gao et al. (2007) reported a decreasing trend in actual *ET* in most areas east of 100° and an increasing trend in the western and northern part of northeast China. Contrary to the general expectations that increase in temperature would increase the actual evaporation, pan evaporation and potential *ET* have been shown to decline in different regions of the world since the 1950s (Chattopadhyay and Hulme, 1997; Chen et al., 2005; Golubev et al., 2001; Hobbins et al., 2004; Lawrimore and Peterson, 2000; Liu et al., 2004; Liu and Zheng, 2004; Peterson et al., 1995; Brutsaert and Parlange, 1998; Thomas, 2000; Roderick and Farquhar, 2002, 2004; Xu et al., 2006). One of the reasons for inconsistent findings in ET_{ref} trends is due to the fact that some climate change studies utilize temperature or radiation-based empirical equations that do not account for other critical climatic parameters such as incoming shortwave or net radiation, wind speed and vapor pressure deficit, potentially providing incomplete or artificial trends and magnitudes in *ET*. The trend in neither *ET* nor evaporation is determined solely by air temperature or solar radiation alone. But, temperature or radiation-based empirical equations treat them as such. Commonly used temperature and radiation-based simplified empirical equations in climate change studies include Thornthwaite (1948), Blaney and Criddle (1950), Makkink (1957), Hamon (1961), Turc (1961), Jensen and Haise (1963), Priestley and Taylor (1972), Linacre (1977), Hargreaves and Samani (1982), and Hargreaves and Samani (1985), which all are deficient in accounting for at least one or more of the key parameters that play a crucial role in determining the trend and magnitude of *ET*.

Since *ET* accounts for over 90% of the total water use in agro-ecosystems (e.g., Nebraska, USA) and accounts for a significant percentage of water use in other ecosystems, accurate estimates of *ET* in studies that investigate the impact of changes in meteorological variables on hydrologic balances is crucial because robust *ET* estimates will play a critical role in better understanding and accurately projecting these impacts on water resources. Despite its crucial importance, unfortunately, ET_{ref} is sometimes poorly addressed in such studies. While physically-based, accurate and robust combination-based energy balance equations such as the Penman or Penman–Monteith, PM (Penman, 1948, 1963; Monteith, 1965), or their derivatives, are available, many models utilize temperature or radiation-based equations to predict potential (reference) *ET* (ET_{ref}). Empirical equations, rather than physically based ones, are often only valid for specific locations, surfaces, or climates and, in a changing climate, for specific time periods. Therefore in trend analysis, empirical equations may need to be recalibrated throughout the period. Using physically-based equations that have been verified in a range of climates should provide more confidence in calculating accurate ET_{ref} values in a changing climate scenario since they have proven accurate in climate conditions similar to those that a location may have. One of the most robust and physically-based equations to estimate ET_{ref} is the Penman–Monteith (PM) reference *ET* equation, which requires net radiation, maximum and minimum air temperature, wind speed, vapor pressure deficit, and maximum and minimum relative humidity to solve for grass- or alfalfa-reference *ET* (ET_o and ET_r, respectively). One common reason for past utilization of temperature or radiation-based empirical equations to estimate ET_{ref} in long-term climate models is the lack of availability of the required input data to solve the combination-based energy balance equations. This practice, however, can introduce significant error and uncertainty in assessing the potential implications of the change in climate parameters on changes in atmospheric evaporative demand, vegetation response, and water balance estimates. Since many climate variables that affect ET_{ref} rates have been changing and are expected to change in the future, single variable equations for estimating the trend in ET_{ref} should be avoided due to the inherent nature of the trend passed to ET_{ref} from the variable. Temperature-based equations provide poor estimates of ET_{ref} because they do not account for net radiation, vapor pressure deficit, or sunshine percentage which can play an important role when calculating ET_{ref}, especially in humid/sub-humid regions where the variations in ET_{ref} are more often due to variations in these factors than to variations in temperature. Similarly, the radiation-based equations, including the Priestley and Taylor (1972), do not account for the impact of the aerodynamic term of the energy balance on ET_{ref}. The lack of ability of the radiation-based equations in accounting for especially the wind speed and relative humidity can impede the performance of these models in windy and rapidly-changing vapor pressure deficit conditions. Thus, effort should be made to integrate methods to be able to solve the combination-based energy balance equations for more accurate ET_{ref} predictions in climate change studies.

This paper presents an integrated approach to solve the combination-based energy balance Penman–Monteith equation for grass- and alfalfa-reference *ET* for a daily time step for a 116-yr period in the Platte River Basin in central Nebraska, USA. Our specific objectives were to demonstrate an approach to estimate key climate parameters (for the period where measurements were not available) such as incoming shortwave radiation, net radiation, relative humidity, saturation vapor pressure, actual vapor pressure, and wind speed on a daily time step to solve the PM equation for

ET_o and ET_r using long-term limited climate data comprising only measured maximum and minimum air temperatures and precipitation. In addition, based on 116-yr of daily data, we attempt to analyze potential changes in climatic parameters and in grass- and alfalfa-reference *ET* on a monthly and annual time steps from 1893 to 2008. We investigate the relationship between ET_{ref} and various climate variables to identify the potential cause(s) of potential changes in trends and magnitude.

2. Materials and methods

2.1. Study location and climate data

Nebraska is one of the leading agricultural states in the USA with over 3.4 million ha of irrigated land and about 5 million ha of natural grassland. The long-term annual (January 1–December 31) statewide average precipitation is about 550 mm. The long-term statewide average growing season (May 1–September 30) rainfall is about 360 mm. The maximum long-term average growing season precipitation occurs in the southeast part of the state and the minimum occurs on the western edge. While a majority of precipitation occurs in spring, the distribution exhibits significant fluctuations within the calendar year. The annual ET_r ranges from about 1400 mm in the southeastern part to 1520 mm in the south central and 1700 mm in the western part of the state. The Central Platte River Basin in Nebraska is one of the largest agro-ecosystem regions with extensive field maize, soybean, seed maize, and irrigated and rainfed grasslands. The dominant cropping system in the region is field maize-soybean rotation with increasing continuous maize production as the demand for ethanol production has been increasing. Most of the croplands in the region are irrigated with center pivots with ground water pumped from the Ogallala aquifer that is the main water supply for irrigation. Irrigation from a shallow ground water supply that is not linked directly to the aquifer is also commonly practiced. Additional vegetation surfaces include a riparian corridor along the Platte River and rainfed croplands. The study location is in a transition zone between sub-humid and semi-arid climatic zones with cold and windy winters and warm and humid summers (Irmak, 2010; Irmak and Mutiibwa, 2010). The wind speed is usually highest during the spring months (March to late May/early June) and in the fall. The long-term (1893–2008) average precipitation is 649 mm, with significant fluctuations between years ranging from 356 mm in 1966 to 999 mm in 2008.

High quality climate data from a weather station located at latitude 41.15°N; longitude 97.97°W; 517 m above mean sea level were used. The station has operated in manual mode from January 1893 to 1987 and in automatic mode since 1987. The High Plains Regional Climate Center (HPRCC, http://www.hprcc.unl.edu) (Hubbard, 1992) serves as a data archive center for the weather stations that were operated by the National Weather Service until 1987. The measured climate data for T_{max}, T_{min}, and precipitation were available on a daily time step from 1893 to 1987. Since 1987, the climate data measured by the HPRCC for the weather station include T_{max}, T_{min}, incoming shortwave radiation, wind speed and direction at 3 m, precipitation, and relative humidity. The instrumentation type and height/depth details of the weather station are given at http://www.hprcc.unl.edu/awdn/instruments/. The HPRCC has a vigorous automatic and routine procedure in place for data quality and integrity checks for days with erroneous and/or missing data (Hubbard et al., 2007). In the trend analyses, linear regression statistics are used to test the statistical significance of the increasing or decreasing trends in the climatic variables and ET_o and ET_r at the 5% significance level.

2.2. The Penman–Monteith grass and alfalfa-reference evapotranspiration equation

We solved the PM equation on a daily time step for grass and alfalfa-reference surfaces. The PM ET_{ref} equation is intended to simplify the presentation and application of the method and associated equations for computing aerodynamic and surface resistance terms where these equations have been combined into a single equation for a daily time step (Irmak et al., 2006, 2008). The PM ET_{ref} equation is essentially same as the original Penman–Monteith equation (Monteith, 1965) with fixed surface resistance values and constant plant height for grass- and alfalfa-reference surfaces (i.e., the surface resistance is 70 s m^{-1} for a grass surface and 45 s m^{-1} for alfalfa). The reference vegetation heights for grass and alfalfa surfaces are considered to be 0.12 and 0.50 m, respectively. The PM ET_{ref} equation as used in this research for daily time step is:

$$ET_{ref} = \frac{0.408\Delta(R_n - G) + \gamma \frac{C_n}{T+273} u_2 (e_s - e_a)}{[\Delta + \gamma(1 + C_d u_2)]} \quad (1)$$

where ET_{ref} = standardized grass or alfalfa-reference *ET* (mm d^{-1}), Δ = slope of saturation vapor pressure versus air temperature curve (kPa °C^{-1}), R_n = net radiation (MJ m^{-2} d^{-1}), G = heat flux density at the soil surface (zero for daily time step), T = mean daily air temperature (°C), u_2 = mean daily wind speed at 2-m (m s^{-1}), e_s = saturation vapor pressure (kPa), e_a = actual vapor pressure (kPa), $e_s - e_a$ = vapor pressure deficit (VPD), γ = psychrometric constant (kPa °C^{-1}), C_n and C_d are numerator and denominator constants that change with reference surface and calculation time step, and 0.408 is a constant in m^2 mm MJ^{-1} ($1/\lambda$, where λ is latent heat of vaporization (2.45 MJ m^{-2} mm^{-1})]. Because of this constant, both R_n and G are in MJ m^{-2} d^{-1} for daily calculations. The C_n value accounts for the time step and aerodynamic resistance of the reference surface. The C_d accounts for the time step, bulk surface resistance, and aerodynamic resistance of the reference surface. The C_n and C_d coefficients, respectively, are 900 and 0.34 for ET_o and 1600 and 0.38 for ET_r for daily time step (Irmak et al., 2006). The next section provides detailed description of assumptions, equations, and procedures used to calculate each climate variable to solve the PM equation for ET_o and ET_r.

2.3. Calculation of unknown meteorological variables for the Penman–Monteith model

2.3.1. Incoming shortwave and net radiation

Measured incoming shortwave radiation (R_s) data were available starting from January 1, 1987 and the R_s values before that date were predicted on a daily basis using the approach proposed by Hargreaves and Samani (1982) and Samani (2000) from T_{max} and T_{min}:

$$R_s = (KT)(R_a)(TD)^{0.5} \quad (2)$$

where $TD = T_{max} - T_{min}$ (°C) and KT is an empirical coefficient (0.162), R_a is daily extraterrestrial radiation (MJ m^{-2} d^{-1}). The estimated R_s values were used in the analyses without local calibration. Daily R_a and other associated variables and parameters were calculated as a function of day of the year, solar constant and declination, and latitude using the procedures presented by (Duffie and Beckman, 1980):

$$R_a = \frac{1440}{\pi} G_{sc} d_r [\omega_s \sin(\varphi)\sin(\delta) + \cos(\varphi)\cos(\delta)\sin(\omega_s)] \quad (3)$$

G_{sc} = solar constant (0.0820 MJ m^{-2} min^{-1})
d_r = inverse relative distance from earth-to-sun
ω_s = sunset hour angle (rad)
φ = latitude (rad)
δ = solar declination (rad)

$$\delta = 0.4093 \sin\left(\frac{2\pi(284+J)}{365}\right) \quad (J = \text{day of the year}, 1\text{—}365 \text{ or } 366) \quad (4)$$

$$d_r = 1 + 0.033 \cos\left(\frac{2\pi J}{365}\right) \quad (5)$$

$$\omega_s = \arccos(\psi) \quad (6)$$

$$\psi = \tan(\varphi)\tan(\delta) \quad (7)$$

We used the following sets of equations to calculate R_n:

$$R_n = R_{ns} \downarrow - R_{nl} \uparrow \quad (8)$$

R_n = net radiation (MJ m^{-2} d^{-1})
R_{ns} = incoming net shortwave radiation (MJ m^{-2} d^{-1})
R_{nl} = outgoing net long-wave radiation (MJ m^{-2} d^{-1}).

The R_{ns} is a result of the balance between incoming shortwave and reflected solar radiation as a function of surface albedo or canopy reflection coefficient (α), which is fixed at 0.23 for green reference surface:

$$R_{ns} = (1 - \alpha) R_s \downarrow \quad (9)$$

Net long-wave radiation is the difference between outgoing long-wave radiation from the earth surface and incident atmospheric long-wave counter-radiation and the rate of R_{nl} is proportional to the fourth power of the absolute temperature of the surface:

$$R_{nl} = \sigma\left[\frac{T_{max,K}^4 + T_{min,K}^4}{2}\right](0.34 - 0.14\sqrt{e_a})\left(1.35\frac{R_s}{R_{so}} - 0.35\right) \quad (10)$$

σ = Stefan–Boltzmann constant (4.903 × 10^{-9} MJ K^{-4} m^{-2} d^{-1})
$T_{max,\ K}$ = daily maximum absolute air temperature (K = °C + 273.16)
$T_{min,\ K}$ = daily minimum absolute air temperature (K = °C + 273.16)
e_a = actual vapor pressure of the air (kPa)
R_{so} = calculated clear sky solar radiation (MJ m^{-2} d^{-1}).

Doorenbos and Pruitt (1977) developed an equation to calculate daily values of R_{so} as a function of station elevation, (z = 517 m for this study), and the extraterrestrial radiation, R_a (MJ m^{-2} d^{-1}) as:

$$R_{so} = (0.75 + 2 \times 10^{-5} z) R_a \downarrow \quad (11)$$

The actual vapor pressure is calculated as:

$$e_a = 0.6108 \exp\left[\frac{17.27 T_{dew}}{T_{dew} + 237.3}\right] \quad (12)$$

where T_{dew} is the dew point temperature (°C). Depending on the availability of data, e_a can be calculated using RH and/or T_{avg}. In the absence of T_{dew}, observations have shown that nightly minimum temperatures tend to be in equilibrium with T_{dew}, thus $T_{dew} \approx T_{min}$ in humid and sub-humid climates. However, this assumption may not always be valid in regions where dew point is not reached regularly (i.e., transitional zones). We computed T_{dew} as (Murray, 1967):

$$T_{dew(i)} = \frac{237.3}{\left[1/\left(\left[\ln\frac{RH_i}{100}/17.27\right]\right) + (T_i/237.3 + T_i)\right]^{-1}} \quad (13)$$

where RH_i = mean relative humidity (%) for period i, and T_i = mean air temperature (T_{max} + T_{min}/2; °C) for period i.

2.3.2. Relative humidity and actual and saturation vapor pressure

Relative humidity from January 1, 1893 to December 31, 1986 was computed as the ratio of the actual vapor pressure (e_a, kPa) to the saturation vapor pressure (e_s, kPa) at the same air temperature:

$$RH = 100(e_a/e_s) \quad (14)$$

The saturation vapor pressure deficit is calculated from measured T_{max} and T_{min}:

$$e_s = \frac{e^o(T_{max}) + e^o(T_{min})}{2} \quad (15)$$

$$e^o(T_{max}) = 0.6108 \exp\left[\frac{17.27 T_{max}}{T_{max} + 237.3}\right] \quad (16)$$

$$e^o(T_{min}) = 0.6108 \exp\left[\frac{17.27 T_{min}}{T_{min} + 237.3}\right] \quad (17)$$

Finally, the only term remaining in Eq. (1) is the slope of the saturation vapor pressure vs. air temperature (Δ), which was calculated as a function of average air temperature as:

$$\Delta = \frac{4098\left[0.6108 \exp\left(\frac{17.27 T_{avg}}{T_{avg}+237.3}\right)\right]}{(T_{avg} + 237.3)^2} \quad (18)$$

The PM equation requires wind speed measurements at 2-m height (u_2, m s^{-1}). The wind speed measured at 3 m from January 1, 1987 to December 31, 2008 was converted to u_2 using the following logarithmic function:

$$u_2 = u_z \frac{4.87}{\ln(67.8z - 5.42)} \quad (19)$$

where u_z is measured wind speed at z meter above the ground (m s^{-1}) and z is the measurement height (m).

2.3.3. Modeling daily wind speed

Wind speed was estimated for the period from January 1, 1893 to December 31, 1986 following the procedures proposed and described by Curtis and Eagleson (1982), in which frequency distributions of wind speeds are considered to be positively skewed and wind speed is treated as a lag-1 Markov process, independent from other climatic variables. The Markov process considers that the value of an event (u_2) at one time is correlated with the value of the event at an earlier period (Gupta, 2008). Similar to approaches presented by Ivanov et al. (2007), in this study the mean and variance of the observed wind speed data (1987–2008) were not allowed to vary with time of the day when estimating wind speed, which would have ensured that the generated values approximate the property of atmospheric stability following a characteristic diurnal curve (Curtis and Eagleson, 1982). The general Markov procedure as outlined by Gupta (2008) comprises: (i) determining statistical parameters from the analysis of historical records, (ii) identifying the frequency distribution of the historical data, and (iii) generating random numbers of the same distribution and statistical characteristics, and constituting the deterministic part considering the persistence (influence of previous u_2 values) and combining the random distribution. To predict daily wind speed data, while preserving the previous distribution of the wind speed, Curtis and Eagleson (1982) suggested that the random term to force skewness on the estimates of the autoregressive model leads to a gamma-type distribution of wind speed. The equation we adopted from Curtis and Eagleson (1982) and Ivanov et al. (2007) for a lag-1 Markov model is:

$$Ws_{(t-1)} = \overline{Ws} + \rho_s(Ws_{(t)} - \overline{Ws}) + \varepsilon_{(t-2)}\sigma_s\sqrt{1 - \rho_s^2} \quad (20)$$

where $Ws_{(t-1)}$ = daily wind speed; $\overline{Ws}$ = mean daily wind speed; ρ_s = lag-1 serial correlation coefficient; σ_s = wind speed standard deviation. The random variable $\varepsilon_{(t-1)}$ was defined as:

$$\varepsilon_{(t-1)} = \frac{2}{\gamma_\varepsilon}\left[1 + \frac{\gamma_\varepsilon \psi_{(t-1)}}{6} - \frac{\gamma_\varepsilon^2}{36}\right]^3 - \frac{2}{\gamma_\varepsilon} \quad (21)$$

where γ_s = skew coefficient of the random variable; $\psi_{(t-1)}$ = standard normal deviate. The skew coefficient of the random variable was defined as:

$$\gamma_\varepsilon = \frac{(1-\rho_s^3)\gamma_s}{(1-\rho_s^2)^{1.5}} \quad (22)$$

where γ_s = skew coefficient determined, just like the other parameters ($\overline{Ws}$, ρ_s, and γ_s) are calculated by the traditional methods, from available observed daily wind speed data for 22-yr period (1987–2008). The standard normal deviate ($\psi_{(t-1)}$) was calculated from standardizing a set of computer generated random numbers using a conventional random number generation algorithm. The daily u_2 was then predicted for the period January 1, 1893 to December 31, 1986.

3. Results and discussion

3.1. Analysis of climate variables: monthly time step

3.1.1. Maximum, minimum, and average air temperature and relative humidity

In this section, the monthly trends of climatic variables (obtained from daily values) that are used in the ET_{ref} calculations are discussed. The trend analyses presented in this study do not account for seasonality in any of the variables. A general change in air temperature can be expected to cause changes in ET_{ref} as well as in other climatic variables; therefore we start our discussions with the trends in temperature. Distribution of T_{max}, T_{min}, and T_{avg}, respectively, from 1893 to 2008 is presented in Fig. 1a–c, respectively. In addition to the trend line, the 10-month moving-average line is also included in the figures. The decadal changes in various meteorological variables from 1893 to 2008 are summarized in Table 1. The decadal trends for each variable in Table were calculated for each 10-yr period to evaluate the decadal changes in variables. The slope of the regression line was multiplied by 10-yr to quantify the magnitude of the change. The 116-yr average trends were also included in Table 1. There is a significant ($P < 0.05$) increasing trend in T_{min} and T_{avg} and increasing, but not significant, trend in T_{max}. The total changes in T_{max}, T_{min}, and T_{avg} over the last 116-yr period were 1.69, 2.84, and 2.26 °C, respectively, with a rate of 0.0136, 0.0236, and 0.0186 °C yr^{-1} (Table 1). Increase in T_{max} and T_{min} usually occurs in the minimum values. The lowest T_{min} occurred on January 12, 1912 as −37.96 °C. The largest warming trend in temperature occurred during 1930s Dust Bowl era when temperatures steadily increased. The greatest T_{max} occurred on July 24 and 25, 1936 as 46.7 °C. The largest decadal increase in T_{max} occurred from 1981 to 1990 and also from 1991 to 2000 as 1.9 °C decade^{-1}. The recent warming trend (1980–2000) is much stronger than during the Dust Bowl era because in the 1930s the sharp increase in air temperature occurred only for 3 yr (1934, 1936, and 1939) whereas the recent warming is steady, especially for the minimum values of T_{min} and T_{max}. The 116-yr average T_{max}, T_{min}, and T_{avg} were 17.14, 3.88, and 10.51 °C, respectively. The largest decadal decrease was observed from 2001 to 2008 as −1.54 °C (slope of T_{max} in Table 1 multiplied by 8 yr, period from 2001 to 2008) when both T_{max} and T_{min} had decreasing trends. The 116-yr average standard deviations for T_{min}, T_{max}, and T_{avg} are 11.4, 12.6, and 11.6 °C, respectively.

3.1.2. Relative humidity and vapor pressure deficit

Distribution of monthly average RH and VPD for 116-yr period is presented in Fig. 1d and Fig. 2a. RH and VPD for the period from 1893 to December 31, 1986 were estimated using Eqs. (14)–(18) and VPD was determined as the difference between e_s and e_a. Measured RH data from January 1, 1987 to December 31, 2008 were used in the analyses. Monthly average RH showed relatively narrow fluctuations in the low (45–55%) range. The monthly average minimum RH is usually around 50–55%. A significant upward shift of the magnitude in RH was observed starting in 1929–1930. There was a 1.84%, and a significant ($P < 0.05$), increase in RH in the last 116-yr period with a rate at 0.0159% yr^{-1}. The largest decline in RH occurred between 1981 and 1990 as 4.71%. The greatest magnitude of increase (2.9%) occurred in three different decades; 1911–1920, 1961–1970, and 2001–2008. The lowest monthly average RH was recorded on September 29, 1952 42.2% and the highest monthly average RH occurred on January 30, 1940 as 80%. The 116-yr monthly average RH is 57.8% and the 116-yr standard deviation is 13.3%. On a 116-yr average, VPD exhibited a relatively constant trend, based on the slope of the regression line (0.000039; Table 1), although there were noticeable upward and downward trends. The greatest VPD values were observed during the Dust Bowl era when annual maximum VPDs were above 4.0 kPa. From 1930s until around 1997, the maximum values of VPD showed a steady decline with some fluctuations, although the average values remained relatively constant, indicating that there were fewer months per year with high VPD values (i.e., higher than 2.0 kPa). VPD had a gradual decline from around 1954 to 2008. The 116-yr average VPD is 0.82 kPa and the 116-yr standard deviation is 0.63 kPa.

3.1.3. Wind speed, incoming shortwave radiation, and net radiation

While we show the trend line in u_2 in Fig. 2b, the trend in u_2 is not expected because in modeling wind speed, the mean u_2 from the whole measured period (1987–2008) was used as the input and the mean value was not varied with season. The modeled (January 1, 1893-December 31, 1986) and measured (January 1, 1987-December 31, 2008) monthly average wind speed is presented in Fig. 2b. Simulated wind speed values for the years 1893–1986 had maximum and minimum daily values of 6.018 and 0.572 m s^{-1} while observed maximum and minimum wind speed values during 1987–2008 were 5.87 m s^{-1} and 0.589 m s^{-1}. Although the algorithm we used simulated wind speed independently of other weather variables, the output values are comparable to the available observed wind speed data of 22 yr (1987–2008) as depicted in Fig. 2b. Although derived independently of other climatic variables, the trends in modeled wind speed values did not exhibit an obvious bias, validating the soundness of the algorithms used in the process. The result indicated that the assumption of autocorrelation affected by the model lag-1 component does exist with day to day variations in wind speed. The wind speed did not exhibit any noticeable trend of increase or decrease. The 116-yr average wind speed is 2.6 m s^{-1} with maximum and minimum values as 8.6 and 0.34 m s^{-1}. The standard deviation of the 116-yr average wind speed is 1.09 m s^{-1}. Based on the slope of the regression line reported on Fig. 2b (0.0002), there was only a slight increase in u_2 as 0.023 m s^{-1} in the last 116 yr.

Overall, there is a significant ($P < 0.05$) decline in R_s and non-significant decline in R_n (Fig. 2c and d). R_s declined with a magnitude of 2.54 MJ m^{-2} mo^{-1} with a rate at −0.0219 MJ m^{-2} mo^{-1}. Decrease in R_n is mainly due to decrease in R_s, which will be discussed in the annual trend analyses section. The maximum monthly average R_n occurred on June 1936 as 16.25 MJ m^{-2} mo^{-1} when the monthly average R_s was 27.28 MJ m^{-2} mo^{-1} with T_{max} close to 39 °C with an RH of 45.6%. The extraterrestrial radiation (R_a) on that month was about 40 MJ m^{-2} mo^{-1}. The minimum monthly average R_n occurred on November 1957 as 0.89 MJ m^{-2} mo^{-1} when the extraterrestrial radiation was one of the minimum values of the year as about 10 MJ m^{-2} mo^{-1} with the R_s value of 8.2 MJ m^{-2} mo^{-1}. The 116-yr average R_n is 7.91 MJ m^{-2} mo^{-1} and the average R_s is 15.9 MJ m^{-2} mo^{-1}. The 1930s drought period is usually associated with maximum values of R_n with values above 14–15 MJ m^{-2} mo^{-1}. The 116-yr standard deviation for daily R_n and R_s, respectively, are

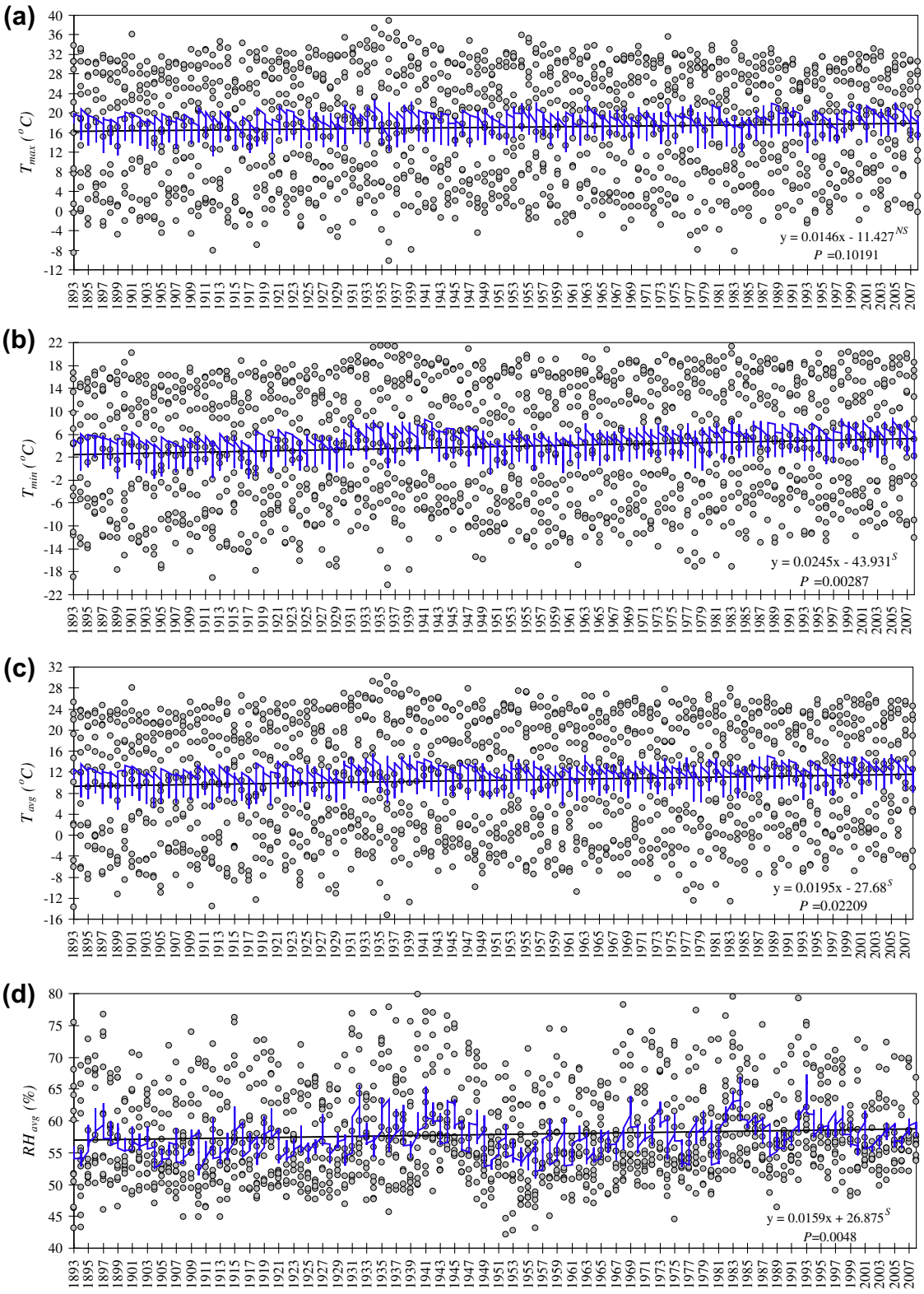

Fig. 1. Monthly average distribution of daily maximum (a), minimum (b), and average (c) air temperature (T_{max}, T_{min}, and T_{avg}), and daily average relative humidity, RH (d) from 1893 to 2008 in the Platte River Basin in central Nebraska, USA (^{S} and ^{NS} indicate that the slope of the regression line is either significant or not significant at the 95% confidence level, $P < 0.05$).

5.02 and 7.5 MJ m^{-2} d^{-1}. It is worth to note that R_n in our study is calculated for a reference surface using albedo = 0.23. Albedo can slightly affect the R_n via its impact on net shortwave radiation. As albedo increases, net shortwave radiation decreases (Eq. (9)) or vice versa. The impact of albedo on ET_o and ET_r is subsidiary as even as high as 20% difference in albedo from 0.23 can cause only 4% and 3% difference in ET_o and ET_r, respectively (Irmak et al., 2010).

Incoming shortwave radiation is one of the key variables used in this study to model R_n and ET_{ref}. As is the case in all modeling studies, modeling R_s from air temperature and R_a has some error that can

Table 1
Trends (unit per 10-yr period) of daily minimum, maximum, and average air temperature (°C), T_{min}, T_{max}, and T_{avg}; precipitation, P (mm); incoming shortwave radiation, R_s (MJ m^{-2}); net radiation, R_n (MJ m^{-2}); wind speed at 2-m, u_2 (m s^{-1}); relative humidity, RH (%); vapor pressure deficit, VPD (kPa); grass-reference evapotranspiration, ET_o (mm); and alfalfa-reference evapotranspiration, ET_r (mm) from 1893 to 2008 in the Central Platte River Basin, Nebraska. The total change in each variable from 1893 to 2008 is included in the last column.

Variable	1893–1900	1901–1910	1911–1920	1921–1930	1931–1940	1941–1950	1951–1960	1961–1970	1971–1980	1981–1990	1991–2000	2001–2008	116-yr(1893–2008)
T_{min}	0.0568	−0.0018	0.0084	−0.0783	−0.0906	−0.2797	−0.0428	0.1041	−0.0877	0.0165	0.0741	−0.0873	0.0236
T_{max}	−0.0272	0.0773	−0.1058	−0.0861	−0.0432	0.0403	−0.0935	−0.0137	−0.0004	0.1964	0.1992	−0.193	0.0136
T_{avg}	0.0149	0.0377	−0.0487	−0.0822	−0.0669	−0.1197	−0.0682	0.0452	−0.044	0.1064	0.1366	−0.1402	0.0186
P	0.017	−0.0405	0.0372	−0.0208	−0.0453	−0.0225	−0.0607	0.0283	−0.0333	−0.0869	−0.0009	0.1254	0.0097
R_s	−0.0735	0.0603	−0.0762	0.0006	0.0223	0.189	−0.0307	−0.0431	0.0385	−0.0546	−0.022	−0.0449	−0.0223
R_n	−0.0367	0.022	−0.0266	0.0043	0.0065	0.0362	−0.0072	0.0045	0.0052	−0.0197	−0.0089	−0.0263	−0.0074
u_2	−0.0054	0.0032	−0.0084	−0.023	−0.0157	−0.0043	−0.0082	−0.0005	0.0192	−0.0084	0.0146	0.0031	0.0002
RH	0.0687	−0.1375	0.2905	0.0718	−0.0515	−0.8035	0.1282	0.2898	−0.201	−0.4708	−0.3451	0.2898	0.0164
VPD	−0.0116	0.0071	−0.0094	−0.0011	0.0041	0.0057	−0.0051	−0.0009	0.0053	0.0123	0.0129	−0.0122	0.000039
ET_o	−0.0271	0.0185	−0.0283	−0.0149	−0.0018	0.0211	−0.012	−0.004	0.0127	0.0219	0.0255	−0.0292	−0.001
ET_r	−0.0384	0.0284	−0.0433	−0.0274	−0.0052	0.0349	−0.0172	−0.0099	0.022	0.0382	0.0418	−0.0419	−0.001

impact the trend and magnitude of changes in ET_{ref}. In Fig. 3, we graphed measured and estimated R_s on a daily basis from January 1, 1987 to December 31, 2008. While the scatter around the 1:1 line is large, the procedures used in this study to estimate R_s on a daily time step is moderate with r^2 of 0.75 with a reasonable root mean square difference (RMSD) of 4.05 MJ m^{-2} d^{-1}. As mentioned earlier, the R_s data were used without any calibration in the R_n and ET_{ref} calculations. The model overestimated considerably in the lower R_s range (i.e., zero to 12–14 MJ m^{-2} d^{-1}) and underestimated at the high R_s range. Most of the large deviations from the 1:1 line are due to the winter (dormant) season R_s estimates that deviated largely from the unity. When monthly average R_s is considered, the relationship between the estimated and measured R_s is stronger (r^2 = 0.95) and RMSD is lower (1.94 MJ m^{-2} mo^{-1}) (data not shown). Overall, the estimates were within 8% (overestimation) of the measured values. On an annual average basis, the estimates were also about 8% greater than the measured values (RMSD = 1.47 MJ m^{-2} yr^{-1}). Overestimation of the R_s would have an impact on the ET_{ref}, but when daily time step is considered, 2% overestimation in R_s would result in only 1% increase in ET_{ref}, when all other meteorological variables remain constant. As mentioned earlier, the error in R_s model estimates was about 8% on a monthly and annual average basis. An 8% increase in R_s (e.g., from 24.6 MJ m^{-2} d^{-1} to 26.568 MJ m^{-2} d^{-1}), while assuming other variables remain the same, results in 2% increase in ET_o and 6.4% increase in R_n. While the R_s model error will have a greater impact on R_n, its impact on ET_{ref} would be subsidiary. Thus, we suggest that while error (overestimation) in the R_s model we used would have an impact on the trends and magnitude of changes in R_n and ET_{ref}, the impact is not expected to be large enough to influence the results of this study considerably when monthly and annual average analyses are considered.

3.2. Analysis of climate variables: annual time step

3.2.1. Precipitation

In the annual trend analyses section, we examine the climatic and environmental factors and variables affecting ET_o and ET_r, and we finally discuss the annual trends in ET_o and ET_r and their relationships with climate variables. In each figure we present the 5-yr-running average as complementary to the slope of the regression line. Decreasing and increasing trends in all variables are more visible on an annual time step as compared with the monthly time step. The annual (January 1–December 31) precipitation varied greatly from year to year. On a long-term average basis (1893–2008) there was a clear and significant ($P < 0.05$) increase in annual precipitation as presented in Fig. 4a. Increase in precipitation can have significant consequences on many other climatic parameters and on ET_{ref}. There was approximately 100 mm of increase in annual precipitation from 1893 to 2008 in the study location at a rate of about 0.90 mm yr^{-1}. Also, there was a significant increase in maximum daily precipitation (the value for the day with the largest amount of precipitation) and a noticeable increase in very heavy or extreme events (i.e., >70 mm d^{-1}) (Fig. 4b). The increase in intense of the rainfall means that there is an increase in precipitation events that may not be beneficial to recharging soil profile due to increase in potential for run-off and flooding. The pattern exhibited by the maximum daily precipitation is generally in-synch (in phase) with the one revealed by the annual total precipitation values. The maximum daily precipitation has increased by about 45 mm between 1893 and 2008 with a rate about 0.40 mm yr^{-1}.

It is clear in Fig. 4a and the 5-yr running averages that from 1893 to 1956 there is a decreasing trend in precipitation and then from 1956 to 2008 the trend become increasing. Daily maximum precipitation events were low from 1893 to 1931 ranging between about 30 to 40 mm d^{-1} and exhibited a sharp increase afterwards. The maximum daily precipitation occurred in 1967 as 123 mm. The 116-yr average precipitation for the study site is 650 mm and 64 out of 116 yrs had above-average precipitation and 50% of the years that had above average precipitation were between 1967 and 2008. The year 2008 had the record high precipitation as 1000 mm. The 116-yr low annual precipitation was in 1966 as 356 mm. Similar to the trends observed in our study other studies have noted the increasing trend, with varying magnitudes, in precipitation and precipitation intensity as well as in stream flow over several North American regions (Lettenmaier et al., 1994; Lins and Michaels, 1994; Karl et al., 1996; Dai et al., 1997; Hulme et al., 1998; Karl and Knight, 1998; Hamelet and Lettenmaier, 1999; Kunkel et al., 1999; Neal et al., 2002; McCabe and Wolock, 2002; Groisman et al., 2004; Gedney et al., 2006; Qian et al., 2007).

3.2.2. Air temperature, incoming shortwave radiation, and net radiation

Maximum air temperature had a non-significant decreasing trend ($P > 0.05$) on an annual time step with a rate of −0.0089 °C yr^{-1} or a total decrease of 1.03 °C for the 116 yr period (Fig. 5a) while T_{min} had a significant ($P < 0.05$) increase with a rate of 0.0382 °C yr^{-1} and a total increase as 4.43 °C for the 116 yr (Fig. 5b). The residuals of average change in all climate variables are presented in Fig. 6. The greatest T_{max} was in 1936 as 46.7 °C and annual average T_{min} was in 1912 as −38 °C. T_{avg} (Fig. 5c) had an increasing trend due to increase in T_{min}, although the rate of increase in T_{avg} is significant and almost 50% less than the rate in T_{min}. Our results are in a very close agreement with those observed by Zheng et al. (2009) who reported an increasing trend in T_{min}, and T_{avg} with a change rate of 0.033 and 0.025 °C yr^{-1} in Haihe

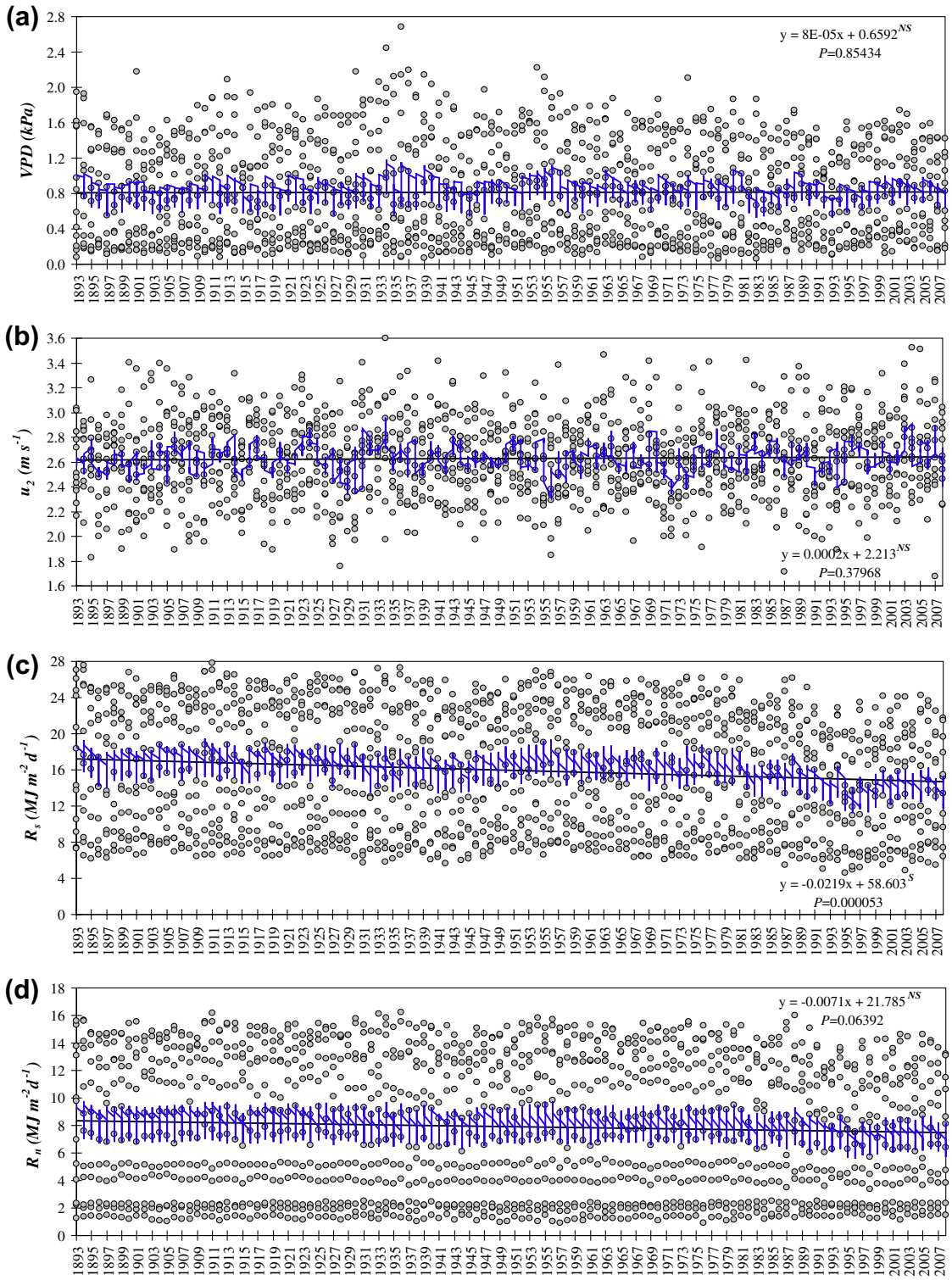

Fig. 2. Monthly average distribution of daily vapor pressure deficit (a), wind speed at 2-m (b), incoming shortwave radiation (c), and net radiation (d) from 1893 to 2008 in the Platte River Basin in central Nebraska, USA (^{S} and ^{NS} indicate that the slope of the regression line is either significant or not significant at the 95% confidence level, $P < 0.05$).

River Basin in China, interestingly with a very similar latitude as our study location.

As expected, R_s followed an opposite trend with precipitation by decreasing significantly with a total amount of -2.59 MJ m^{-2} 116-yr^{-1} or with a rate of -0.022 MJ m^{-2} yr^{-1}. Net radiation (Fig. 5e) followed a similar trend as R_s with a lesser magnitude of decrease. Zheng et al. (2009) found similar results as decrease in R_s at a rate of -0.023 MJ m^{-2} d^{-1} yr^{-1}. The maximum annual average R_s occurred in 1956 as 17.5 MJ m^{-2} d^{-1} (almost the same value as observed in 1894). Although 2008 had the record high precipitation in the last 116-yr period, the minimum R_s occurred in 1995. R_n also decreased significantly with a rate of -0.0032 MJ m^{-2} yr^{-1}. The maximum and minimum R_s and R_n did not always follow each other. For instance, while maximum R_s was in 1956 the maximum

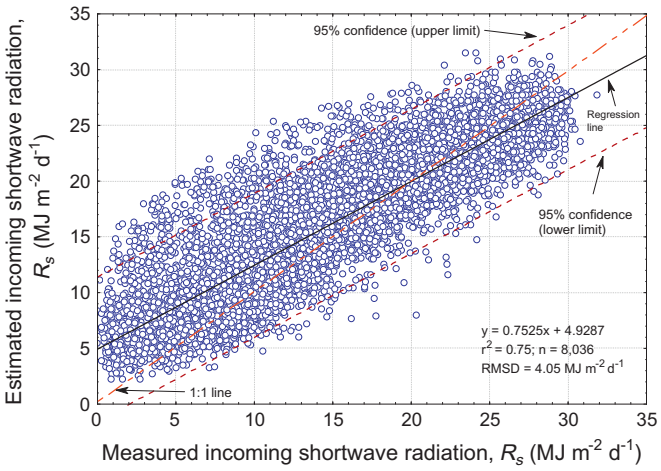

Fig. 3. Estimated vs. measured incoming shortwave radiation from the measurement period of January 1, 1987 through December 31, 2008.

R_n occurred in 1988. Increases in T_{min} and decreases in T_{max} along with increasing precipitation are consistent with the reduction in daily temperature ranges observed on cloudy days. Minimum temperatures usually occur during the nighttime, and cloudy nights are characterized by greater net longwave radiation near the surface resulting in greater minimum temperatures (greenhouse effect). Maximum temperatures typically occur during the daylight hours, and cloudy skies reduce R_s resulting in lower T_{max}. This can be characterized by asymmetric warming of a climate influenced by increased cloudiness (Balling and Idso, 1990; Moot et al., 1996; Moonen et al., 2002) and precipitation as shown in Fig. 4a and b. The opposite trends found in T_{max} from daily values versus annual averages may be indicative of a change in the number of days that have maximum and minimum T_{max} values (similar to the opposite trends in VPD_{avg} vs. VPD_{max}, Fig. 6h vs. i). Just as the distribution of precipitation events has changed, the distribution of T_{max} has changed. It is important to note that climate change may not always be characterized by changes in the means of the climate variables, rather other climate descriptors, such as the standard deviations, skewness, or medians and modes of a variable, may also change.

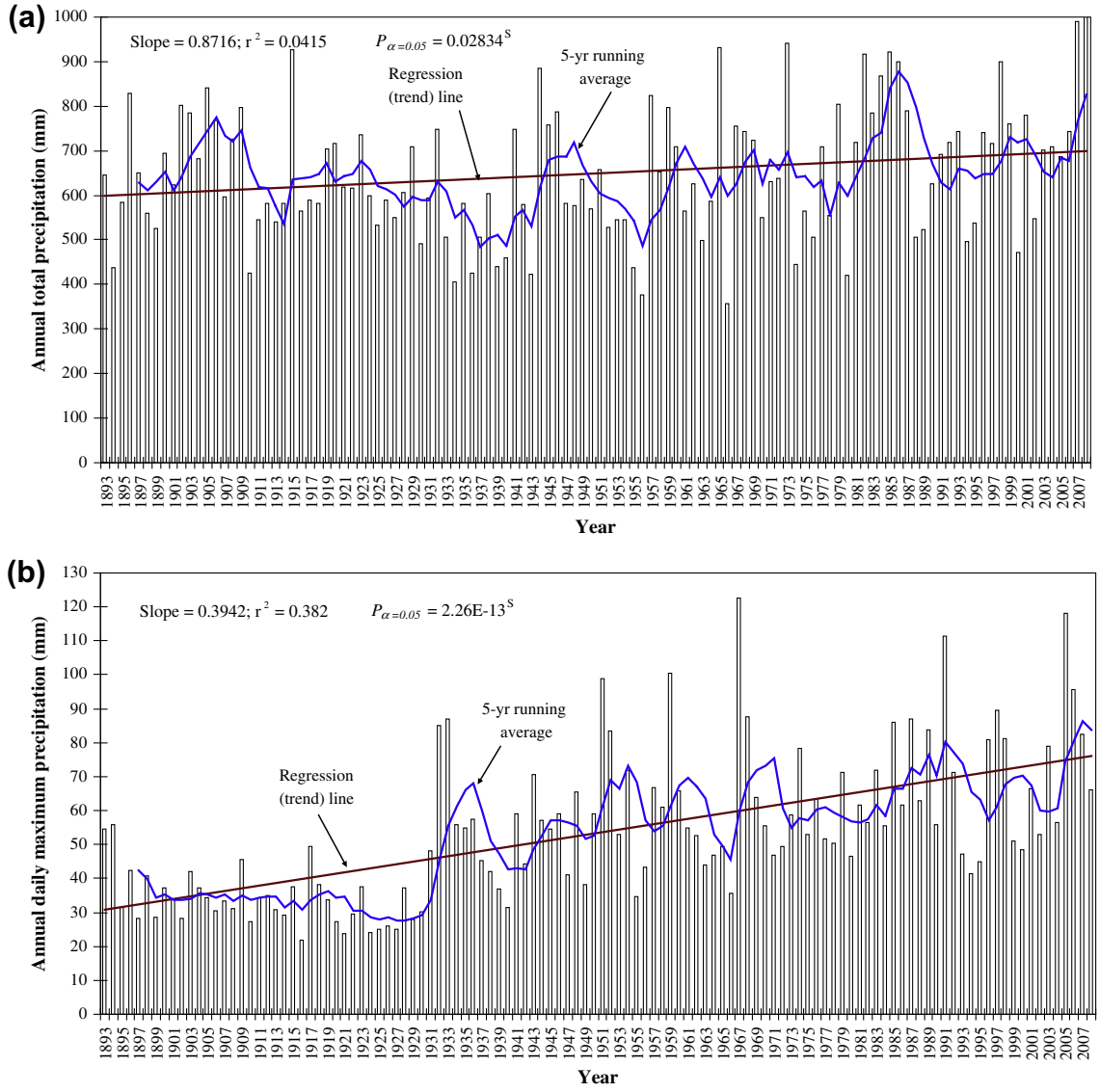

Fig. 4. Annual total precipitation (a) and annual daily maximum precipitation in a given year (b) from 1893 to 2008 in the Platte River Basin in central Nebraska, USA (^{S} indicates that the slope of the regression line is significant at the 95% confidence level, $P < 0.05$).

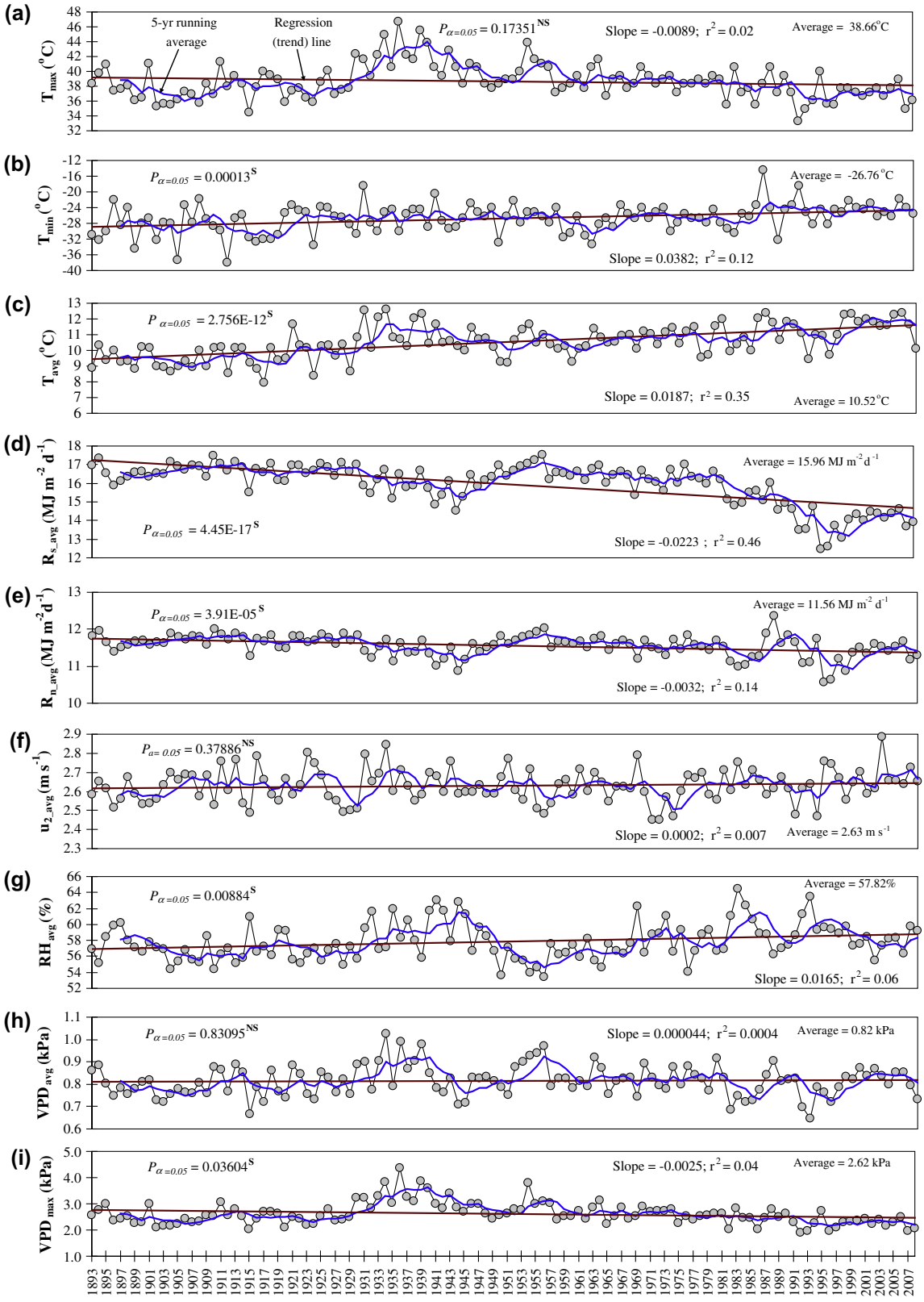

Fig. 5. Average changes in climatic variables [maximum air temperature, T_{max} (a); minimum air temperature, T_{min} (b); average air temperature, T_{avg} (c); incoming shortwave radiation, R_s (d); net radiation, R_n (e); wind speed at 2 m, u_2 (f), relative humidity, RH (g); vapor pressure deficit, VPD (h), and maximum VPD (i)] on an annual time step from 1893 to 2008 in the Platte River Basin, Nebraska, USA (^{S} and ^{NS} indicate that the slope of the regression line is significant or not significant at the 95% confidence level).

3.2.3. Wind speed, relative humidity, and vapor pressure deficit

Wind speed (Fig. 5f) remained relatively constant throughout the 116-yr period with a slight, and insignificant ($P > 0.05$), increase at a rate of 0.0002 m s^{-1} yr^{-1} or 0.023 m s^{-1} 116-yr^{-1}. The two sharpest decreases in u_2 are clearly visible between 1923 and 1928 as 0.3 m s^{-1} and from 1969 to 1971 with the same magnitude. While our analyses of wind speed do not consider seasonal trends, Cohen et al. (2002) reported an increase in wind

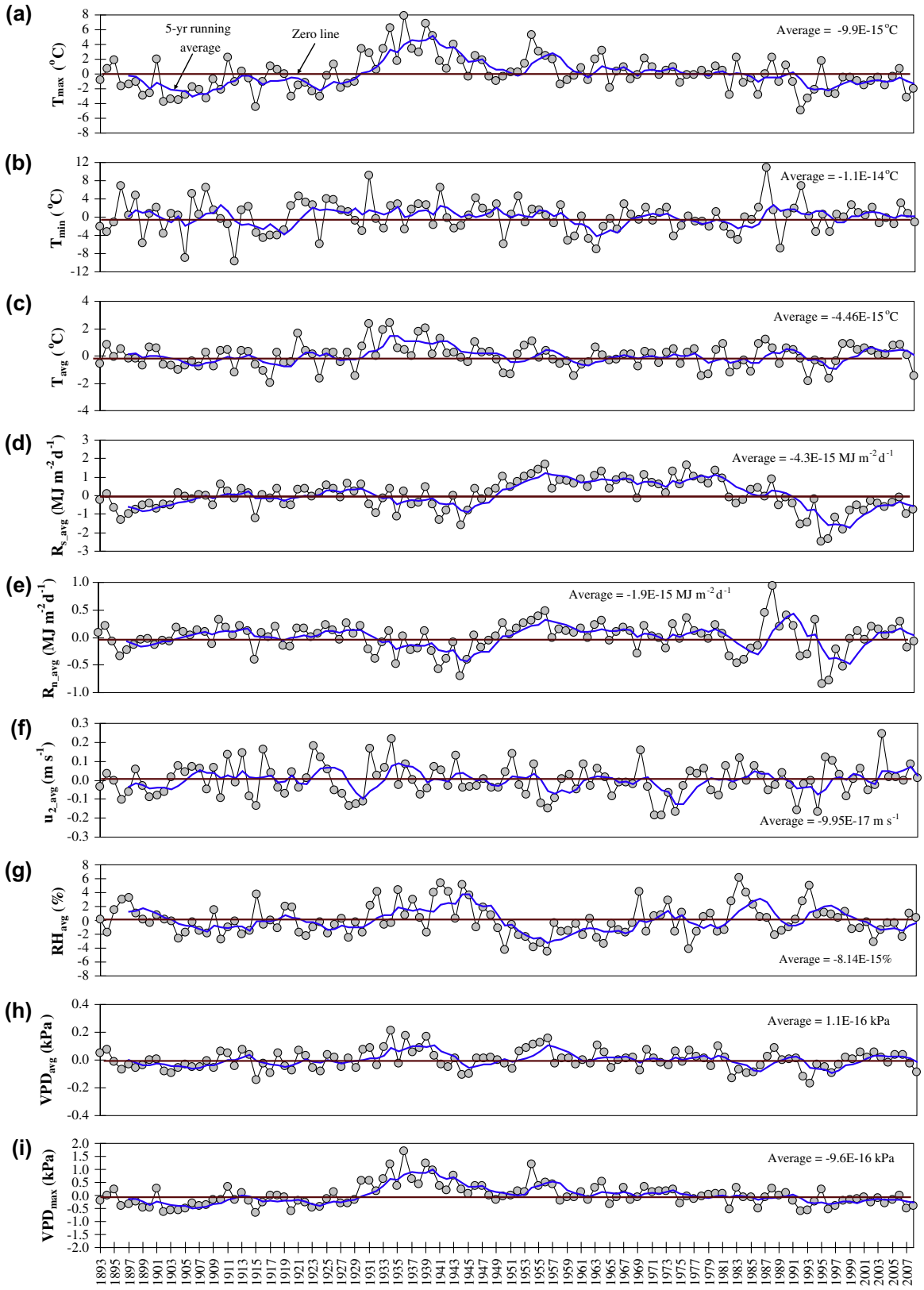

Fig. 6. Residuals of average changes in climatic variables [maximum air temperature, T_{max} (a); minimum air temperature, T_{min} (b); average air temperature, T_{avg} (c); incoming shortwave radiation, R_s (d); net radiation, R_n (e); wind speed at 2 m, u_2 (f), relative humidity, RH (g); vapor pressure deficit, VPD (h), and maximum VPD (i)] on an annual time step from 1893 to 2008 in the Platte River Basin in central Nebraska, USA.

speed for Bet Dagan, Israel, which usually occurred in the summer and autumn months. They reported that between May and November wind speeds increased by up to 0.025 m s^{-1} each year, mainly in the afternoon hours wind speeds. They also reported significant wind direction changes during the same months as wind directions veered clockwise by about 1° annually. Yin et al. (2010) observed a

significant decline in wind speed at a rate of −0.09 m s^{-1} per decade in China with a relative change of −23.74%. Zheng et al. (2009) observed a considerable decrease in u_2 at a rate of −0.014 m s^{-1} yr^{-1}. It can be expected that a decrease in u_2 would induce ET_{ref} to decline under the assumption that the other meteorological variables that drive ET_{ref} remain constant, which is almost never the case. Impact of u_2 on ET_{ref} can easily be offset by changes in other variables, especially changes in R_s.

As a result of increase in precipitation, RH (Fig. 5g) decreased significantly by 1.9% 116-yr^{-1} with a rate of 0.0165% yr^{-1}, which is close to the value found by Yin et al. (2010) who observed an insignificant decreasing trend in RH at a rate of only −0.34% per decade with a relative change of −2.25%, which was the smallest change within the five meteorological variables (wind speed, sunshine hour duration, T_{max}, T_{min}, and RH) they evaluated. In general, the annually average VPD (Fig. 5h) followed an opposite trend to RH and remained relatively constant, although with large fluctuations in the 1930s, 1950s, and 1980s, with a slight increasing trend at a rate 0.00004 kPa yr^{-1} or 0.005 kPa 116-yr^{-1}. On an annual time step, the correlation between RH and VPD is not strong (r^2 = 0.30, data are not shown) because the same meteorological and surface parameters influence both variables differently. For instance, increased precipitation can increase RH, but reduces VPD. Annual average maximum VPD (Fig. 5i) had a significant decreasing trend at a rate of −0.0025 kPa. The maximum annual average VPD occurred in 1936 as 4.35 kPa when T_{max} was at its maximum (46.7 °C) in the 116-yr period.

3.3. Analysis of grass and alfalfa-reference evapotranspiration

Daily distribution of ET_o and ET_r is presented in Fig. 7a and b. The annual total values are presented in Fig. 8a and b. The P value, slope and the 5-yr running average are included in Fig. 8a and b. Both ET_o and ET_r had significant ($P < 0.05$) decrease on a daily time step. The maximum daily ET_o and ET_r occurred on the same day (July 17, 1936) as 11.9 mm and 16.9 mm. Daily ET_o and ET_r decreased at a rate of −0.001 mm d^{-1}. On an annul time step both ET_o and ET_r declined, but only the decline in ET_o was significant ($P < 0.05$). Both ET_o and ET_r decreased at a rate 0.36 mm yr^{-1}. ET_r had much larger fluctuations than ET_o and this may be the reason for a non-significant decline in ET_r. Annual total ET_o ranged from 1003 mm in 1993 to 1377 mm in 1934. ET_r ranged from 1351 mm in 1993 to 1885 mm in 1934. Year 1993 was a very wet year [774 mm precipitation with one of the lowest annual average T_{max}, R_s, with a second highest annual average RH (63.5%), with a lowest annual average VPD (0.65 kPa) and the lowest maximum VPD (1.95 kPa)] (Fig. 5). Year 1934 had the highest annual average u_2, second highest T_{max}, highest T_{avg}, highest average and maximum VPD (Fig. 5). The observed decreasing rate in ET_{ref} (0.36 mm yr^{-1}) is less than those reported in the western and eastern USA, (Peterson et al., 1995), Australia (Roderick and Farquhar, 2004); the Tibetan Plateau in China (Zhang et al., 2007), the Yangtze River Basin (Xu et al., 2006), and the Haihe River Basin in China (Zheng et al., 2009). Chattopadhyay and Hulme (1997) observed that the potential ET decreased up to a maximum of 0.30 mm d^{-1} decade^{-1} over west-central India in the monsoon and post-monsoon seasons. The lower magnitude of rate of decrease in ET_{ref} in our study is largely due to considering a point scale ET_{ref} whereas the aforementioned studies mostly considered the trends in ET_{ref} rates on a basin and/or regional scale. Differences are also due to using different approaches to compute ET_{ref}.

While both ET_o and ET_r are very powerful indicators of collective changes in climate variables on atmospheric evaporative demand as integrated by the Penman–Montieth model, worldwide, ET_o is more commonly used than ET_r. In theory and in practical application, there is no difference in choosing one reference surface over the other. Ideally, using ET_o or ET_r to quantify evaporative demand and actual ET should result in similar conclusions as to the magnitudes and trends. There is no consensus on which reference surface should be chosen for a particular region, but the choice could be a function of climate characteristics of a local region or location. For example, ET_r may be preferable for semi-arid or arid climates because alfalfa tends to transpire water at potential rates even under advective environments. Also, alfalfa has a vigorous and deeper root structure and is, therefore, less likely to suffer water stress compared with a shallow-rooted grass. In places such as humid, sub-tropical climates where alfalfa is not commonly grown the grass-reference may be preferable (Irmak et al., 2008). More vigorous root structure and higher rate of transpiration attributes of alfalfa-reference, which are implicitly embedded in the calibration parameters in Eq. (1) as compared with the grass-reference surface, may be the likely reasons for the larger fluctuations and insignificant decline in ET_r in Fig. 8a. Also alfalfa has greater aerodynamic and lower surface resistance than a grass surface (70 s m^{-1} for grass and 40 s m^{-1} for alfalfa). Thus, while using ET_o or ET_r would result in similar or same actual ET values for a specific vegetation surface, given the fact that grass is slightly more sensitive to changes in meteorological variables, its use may be preferred in evaluating the impact of changes in climate variables on ET_{ref}.

Since both reference surfaces can be used in climate studies in determining atmospheric evaporative demand and in estimating actual ET (ET_a) rates of vegetation surfaces using a one-step approach of adjusting ET_{ref} with crop coefficients (K_c), in some cases ET_o needs to be converted to ET_r, or vice versa, so that the K_c values developed for one surface can be used with the other surface to estimate ET_a for a specific plant surface (i.e., $ET_a = ET_{ref} \times K_c$). This approach is a very commonly used approach in estimating ET_a rates of agronomical vegetation and has the potential to be used in climate change and hydrologic studies because as climate changes, land use (i.e., the type and nature of the vegetation) could change as well and ET_{ref} can be linked to surface via K_c to estimate ET_a on large scales. Since grass or alfalfa-based K_c values are not interchangeable [i.e., K_c values that were developed using ET_o (K_{co}) cannot be used with ET_r to estimate ET_a] the conversion factor between ET_o and ET_r is needed. While changes with the season and other factors can vary between the locations, we found that on a calendar year basis, the long-term average ET_r to ET_o ratio is 1.35 (Fig. 9). Irmak et al. (2008) found that the ET_r/ET_o ratio varies less during the growing season (May–September) than the non-growing (dormant) season. They also reported that the average standard deviation between long-term average data was a maximum of only 0.13 for the calendar year and a maximum of 0.10 for the growing season when using Eq. (1) to develop the ratios. Irmak et al. (2008) reported long-term monthly average ET_r/ET_o ratios and their standard deviations for several locations. Regardless of the reference surface used, the ratio (1.35) reported in this study is useful to make conversions between ET_r and ET_o in the climate change studies.

3.4. Relationships between reference evapotranspiration and meteorological variables

Contrary to the expected increasing trend in ET_{ref} due to well-established increasing trends in air temperature, many studies (Peterson et al., 1995; Chattopadhyay and Hulme, 1997; Brutsaert and Parlange, 1998; Lawrimore and Peterson, 2000; Roderick and Farquhar, 2002, 2004; Chen et al., 2005; Xu et al., 2006) have shown that ET_{ref} as well as pan evaporation, which is strongly correlated to ET_{ref}, have decreased in many regions of the world. As reported by Yin et al. (2010) several studies attributed decreasing trends to decreased sunshine duration or R_s in Russia and USA (Peterson et al., 1995), China (Thomas, 2000; Liu et al., 2004; Gao

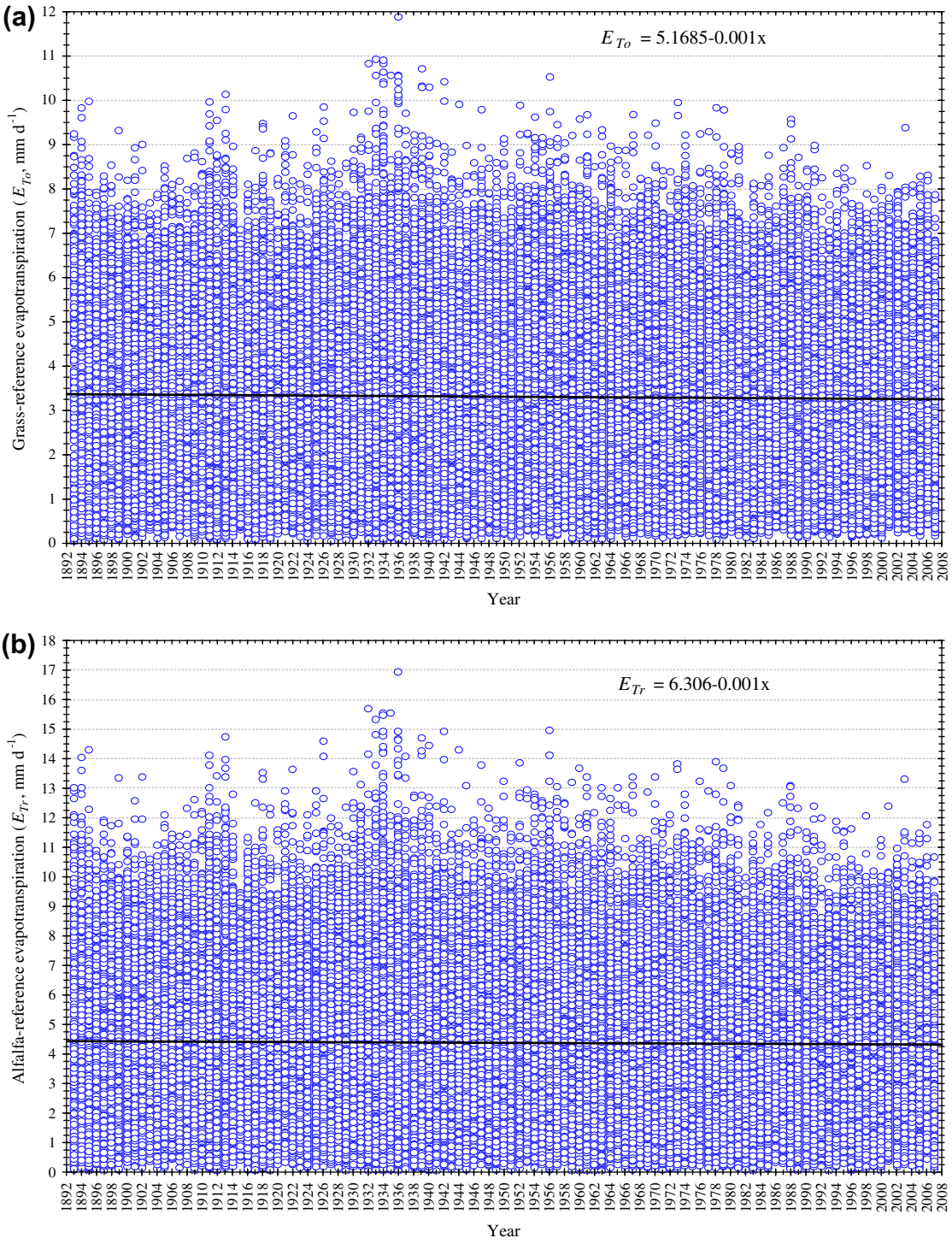

Fig. 7. Distribution of daily grass (ET_o) (a) and alfalfa (ET_r) (b) reference evapotranspiration from 1893 to 2008 in the Platte River Basin in central Nebraska, USA.

et al., 2006; Wang et al., 2007), Israel (Cohen et al., 2002), and, in general, in the Northern Hemisphere (Roderick and Farquhar, 2002). The decrease in ET_{ref} was attributed to wind speed in Australia (Rayner, 2007; Roderick et al., 2007), the Tibetan Plateau (Chen et al., 2006; Zhang et al., 2007), and Canada (Burn and Hesch, 2007). Chattopadhyay and Hulme (1997) attributed the decrease in ET_{ref} in India to an increase in RH. Cong and Yang (2009), Ohmura and Wild (2002), and Xu et al. (2006) attributed the decrease in ET_{ref} to air temperature. Ren and Guo (2006), Gao et al. (2006), and Xu et al. (2006) attributed the decrease in ET_{ref} to a combination of changes in R_s and u_2. There is no consensus among scientists as to what meteorological variable(s) have caused decreases in ET_{ref}, which is expected because the impact of individual meteorological variable(s), especially the impact of their interactions on ET_{ref}, can change substantially from one region to another and even in the same region can change temporally and spatially. Thus, the sensitivity of ET_{ref} to climate variables can show significant variation between the locations as well as between the years within the same location. This is especially true when ET_{ref} is calculated using a combination-based energy balance method (i.e., Penman–Monteith) that integrates the effect of various climate variables on ET_{ref}.

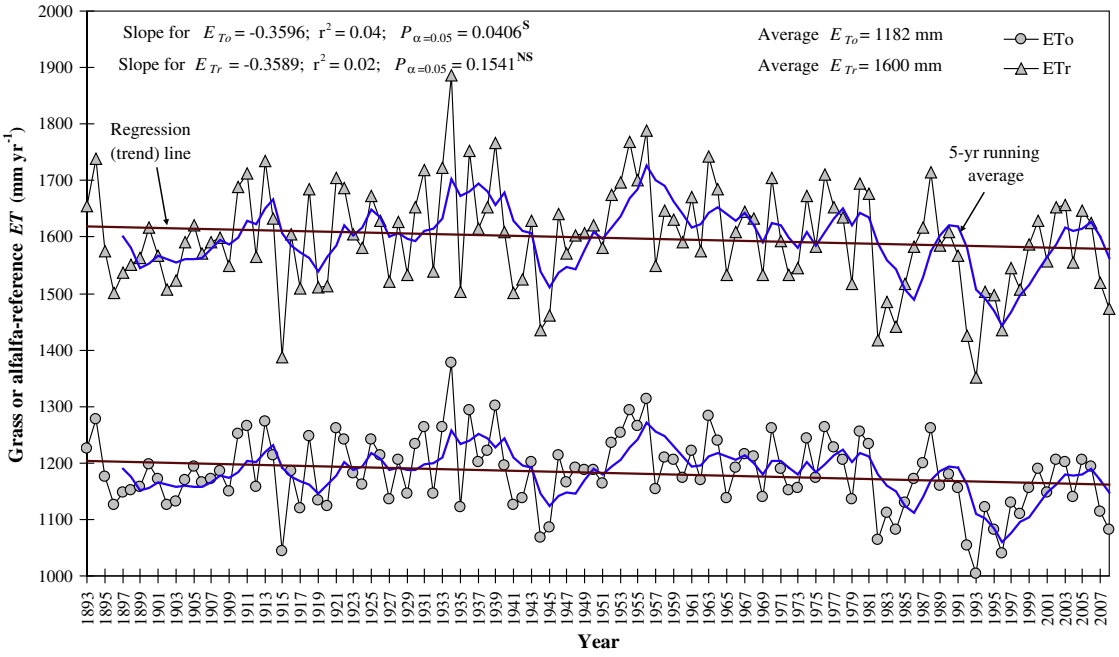

Fig. 8. Annual totals of grass and alfalfa-reference evapotranspiration (ET_o and ET_r) from 1893 to 2008 in the Platte River Basin in central Nebraska, USA (^{S} and ^{NS} indicates that the slope of the regression line is significant and not significant at the 95% confidence level).

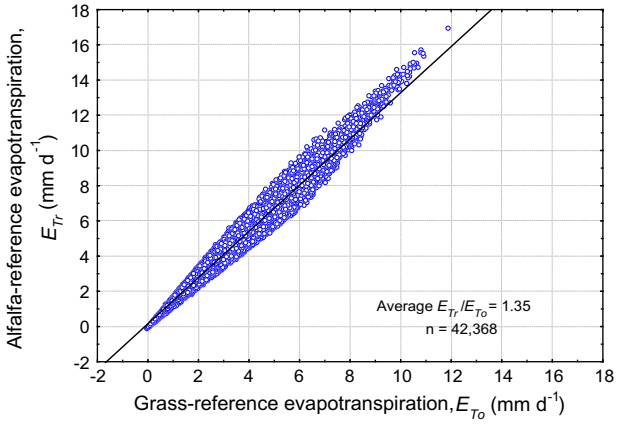

Fig. 9. Daily alfalfa-reference evapotranspiration (ET_r) vs. grass-reference evapotranspiration (ET_o) from 1893 to 2008 in the Platte River Basin in central Nebraska, USA.

On an annual time step, we analyzed the relationships between ET_{ref} and climate variables to potentially determine the main parameters that caused decrease in ET_{ref}. We correlated only ET_o to various climate variables as the relationships would be either the same or very similar for ET_r. The relationships between ET_o and precipitation (P), T_{max}, T_{min}, T_{avg}, RH, VPD_{avg}, u_2, R_s, and R_n are presented in Fig. 10a–i. On an annual time step, ET_o significantly ($P < 0.05$) correlated to P, T_{max}, T_{avg}, RH, VPD_{avg}, R_s, and R_n. ET_o did not respond to changes in T_{min} or u_2 (Fig. 10c and g). The ET_o most highly correlated to VPD_{avg} ($r^2 = 0.84$). Change in ET_o is also strongly correlated to R_n with $r^2 = 0.52$, which is higher than the r^2 of any other variable, except VPD. This can have a significant implication in terms of empirical equations that are commonly used in climate change studies that do not account for R_n. Especially temperature-based equations will provide poor estimates of ET_{ref} mostly because they do not account for R_n and VPD, which play crucial role when calculating ET_{ref}, especially under humid regions where the variations in ET_o are more often due to variations in these factors than to variations in temperature.

Decline in ET_o with increasing P (Fig. 10a) is expected as an increase in P is usually associated with increase in cloudiness and decrease in R_s, R_n, T_{max} and, VPD. Precipitation is significantly ($P < 0.05$) correlated to VPD_{avg} ($r^2 = 0.42$), T_{max} ($r^2 = 0.27$), R_n ($r^2 = 0.24$), and RH ($r^2 = 0.21$) (data are not shown). The increasing air temperature causes a simultaneous increase in both VPD and outgoing long-wave radiation (Eq. (10)). The increase in VPD increases advective water transfer; while the decrease in R_s reduces R_n. In our study, RH increased significantly and VPD decreased due to increases in air temperature and precipitation, contributing to atmospheric moisture, and a decrease in R_s. As indicated in Fig. 5 T_{min}, T_{avg}, u_2, and VPD all had an increasing trend and contributions to increasing ET_{ref}. However, the affect of increases in these variables have been offset by the decrease mainly in R_s, due to increases in precipitation and cloudiness. One variable is not solely responsible in driving the trend and magnitude of ET_o. For instance, while ET_o did not respond to changes in T_{min} alone, a significant increase in T_{min} causes a significant increasing trend in T_{avg}, which ultimately increases VPD. While the correlation between ET_o and VPD is much stronger than correlation between ET_o and RH, significant increase in RH resulted in marginal increase in VPD that would have been much greater otherwise due to a significant increase in air temperature. Although it was not significant, the reduction in u_2 may be an indication of weakening of regional atmospheric circulation, thereby decreasing ET_{ref}. However, this may not always be the case because, mechanistically, the impact of u_2 on ET_{ref} is also a strong function of the moisture content of the air that is carried over the surface with wind. If the air that is saturated above the surface is replaced with a drier air carried by wind this would increase the atmospheric demand and increase ET_{ref}, which can be a usual case in arid and semi-arid climates. If the saturated air above the surface is replaced with more humid air, the impact of u_2 on ET_{ref} may be marginal, which is usually the case in humid climates. In our study, although the trend in u_2 was not significant it implicitly impacts the ET_{ref} and is accounted for in the Penman–Monteith equation. In addition, there is an impact of these variables on the length of the growing season which is an important consideration when assessing the trends in annual ET_{ref} totals. For example, greater ET_{ref}

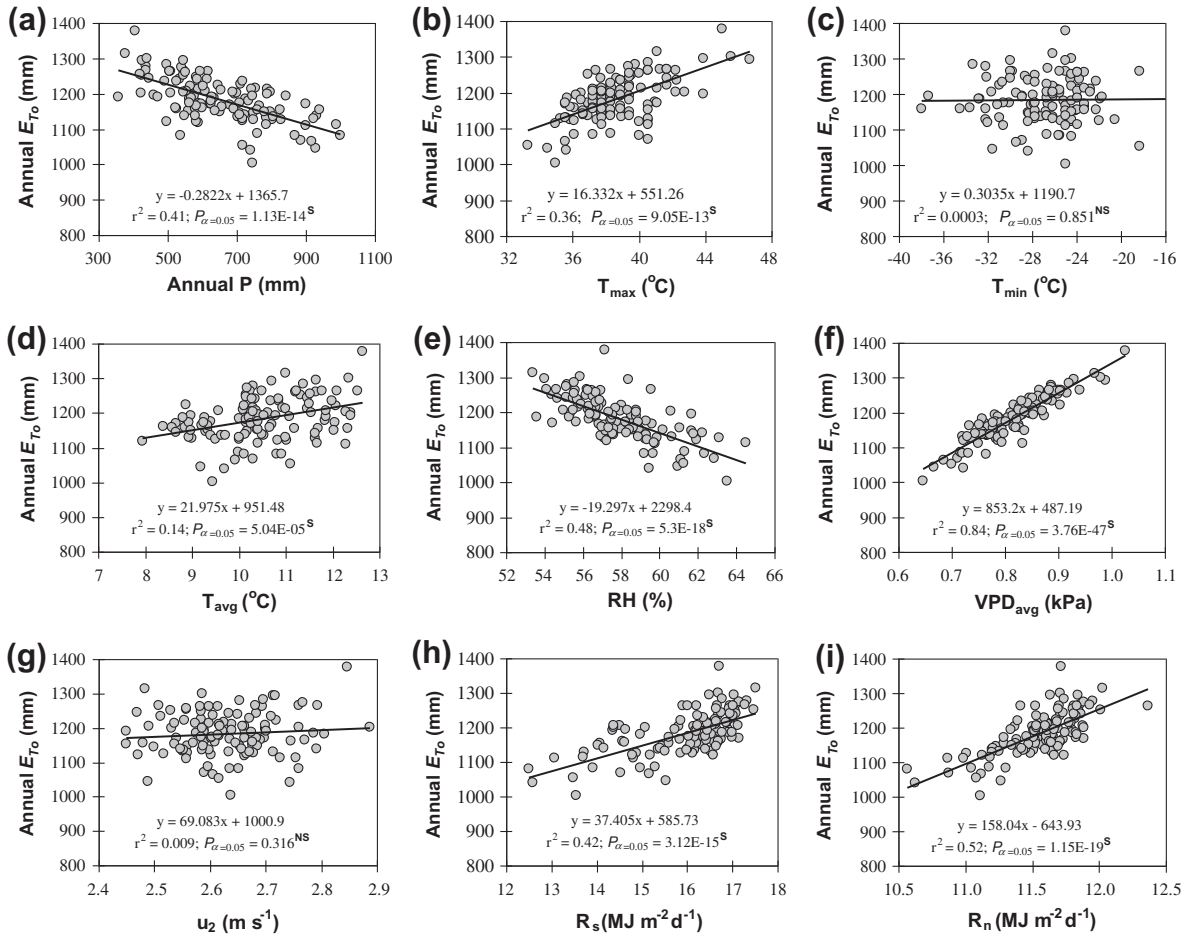

Fig. 10. Relationship between grass-reference evapotranspiration (ET_o) and precipitation, P (a); maximum air temperature, T_{max} (b); minimum air temperature, T_{min} (c); average air temperature, T_{avg} (d); relative humidity, RH (e); vapor pressure deficit, VPD_{avg} (f); wind speed at 2 m, u_2 (g); incoming shortwave radiation, R_s (h); and net radiation, R_n (i) on an annual time step from 1893 to 2008 in the Platte River basin, Nebraska, USA (^{S} and ^{NS} indicate that the slope of the regression line is significant or not significant at the 95% confidence level).

rates may occur during parts of the growing season but if the length of the growing season decreases, yearly ET_{ref} totals may decrease. Follow up work by the authors is currently investigating seasonal changes in ET_{ref} and thermal units (growing degree days) and their implications on ET_a and agricultural productivity at five locations in the Great Plains of the United States.

Higher sensitivity of ET_o to VPD and R_n (Fig. 10f and i) than to other variables, in these study conditions, is consistent with previous research. In a study that investigated the sensitivity of the PM equation (Eq. (1)) to various climate variables in a semi-arid, Mediterranean-type climate, coastal humid, inland humid, semi-humid, and an island regions, Irmak et al. (2006) found that, in general, ET_o was most sensitive to VPD at all locations [Scottsbluff, NE (semi-arid); Bushland, TX (arid/semi-arid); Santa Barbara, CA (Mediterranean climate); Fort Pierce, FL (humid coastal); Rockport, MO (humid inland); Clay Center, NE (sub-humid); and Twitchell Island, CA (island)). However, sensitivity of ET_o to the same variable showed significant variation from one location to another and at the same location within the year. After VPD, ET_o was most sensitive to u_2 at semi-arid regions with strong winds. The R_s was the dominant driving force of ET_o at humid locations. At semi-arid and island locations ET_o was more sensitive to T_{max} than R_s in summer months, whereas it was equally sensitive to T_{max} and R_s at semi-humid locations. The ET_o was not sensitive to T_{min} at any of the locations. Increase in ET_o with respect to increase in climate variable varied temporally. These findings indicate that each climate variable has an important role to play in the trend and magnitude and their roles change with regional characteristics. Thus, only one or two meteorological variables cannot be responsible for the trend and magnitude of ET_{ref} and they all need be collectively accounted for in a combination-based energy balance equations, rather than temperature or radiation-based simplified empirical equations, when used in climate change studies.

While it is not our intention to extrapolate the decline in ET_{ref} found at this location to other locations or to actual ET of non-reference surfaces, we find it important to compare our trends to trends in actual ET found in other studies, particularly in regard to the "pan-evaporation paradox", which was first introduced by Brutsaert and Parlange (1998). The paradox describes the seeming contradiction of decreases in pan-evaporation alongside increases in air temperature. Several studies explain this paradox and conclude increasing trends in actual ET by citing a complementary relationship between pan or potential ET and actual ET, where increases in actual ET follow increases in temperature which result in decreases in VPD and increases in cloudiness leading to declines in pan and potential ET (Lawrimore and Peterson, 2000; Golubev et al., 2001; Kahler and Brusaert, 2006). Brutsaert and Parlange (1998) limit this explanation to locations that are water limited, i.e., water availability rather than energy availability controls actual ET rates. For this study, we do not believe that the decreasing trend for ET_{ref}, which is an estimation of the actual evapotranspiration from a non-water-limited reference surface, is contradictory

to the increasing *ET* trends found in other studies. Qian et al. (2007) found that simulated evapotranspiration rates increased at 32.4 mm century^{-1} over the Mississippi River Basin, with a sensitivity analysis suggesting that the majority of the increase was due to an increase in precipitation which was partially offset ($-$23.5 mm century^{-1}) by a reduction in solar radiation due to cloud cover. The increase in *ET* in their study could be related to the higher level of moisture provided by increase in precipitation, however. The difference in our study is that we have quantified that trend at a single non-water limited location in the Platte River Basin, so our results are consistent with this result in that increases in precipitation to a reference surface would not necessarily increase actual evapotranspiration rates. Rather evapotranspiration rates from a non-water limited surface may be hindered by increases in precipitation at the same time as available energy is decreasing, as we found in this study. In addition, a large amount of increase in precipitation found here was in heavy precipitation events which may not remain at that location to be effectively used for actual *ET* due to potential increases in run-off events. We suggest that trends in actual evapotranspiration rates are not just regional, as shown in other studies (Trenberth et al., 2007; Huntington, 2006), but have a highly local dependency. ET_{ref} declines will depend on many factors, including regional and surface characteristics, and interactions of climatic and vegetation parameters. Furthermore, ET_{ref} and actual *ET* are driven primarily by similar energy terms of the atmospheric factors that determine evaporative demand. Since actual *ET* will be impacted more by the surface (e.g., soil, topography, and hydrology), and perhaps more importantly by the vegetation characteristics, the trend and magnitude of change in actual *ET* will be a strong function of local surface characteristics. Thus, the local characteristics will primarily dictate the direction of change in ET_{ref} and actual *ET* and their relationship to pan evaporation.

4. Summary and conclusions

Here, although we found a significant ($P < 0.05$) increasing trend in both T_{min} and T_{avg} at a rate 0.038 °C yr^{-1} and 0.0187 °C yr^{-1}, respectively, and insignificant increasing trend in u_2 and VPD, we observed a significant ($P < 0.05$) decline in estimated ET_{ref} ($-$0.3596 mm yr^{-1} for ET_o and $-$0.3586 mm yr^{-1} for ET_r). We presented analyses that suggest the decrease in ET_{ref} is most likely due to significant increase in precipitation that results in significant reduction in R_s and R_n as available energy is the primary driver of ET_{ref}. Since VPD and u_2 remained relatively constant in the last 116-yr period, we attribute the decrease in ET_{ref} to the decrease in R_s and, in turn, decrease in R_n, at our study location. There was approximately 100 mm of increase in precipitation from 1893 to 2008 in the study location at a rate of about 0.90 mm yr^{-1}. Also, there was a significant increase in maximum daily precipitation, especially in the very high events (i.e., >70 mm d^{-1}). We present detailed analyses of relationships between ET_{ref} and all meteorological variables and sensitivity of ET_o to the variables. On an annual time step ET_{ref} significantly ($P < 0.05$) and inversely correlated to precipitation and RH, and significantly and positively correlated to T_{max}, T_{avg}, VPD, R_s, and R_n.

In some studies that investigate the relationships between changes in climate variables and hydrologic balances and their impact on water resources, ET_{ref} is calculated using mean air temperature- or radiation-based empirical equations. For example, temperature-based equations have been predicting increases in ET_{ref} in locations where temperatures have been increasing, by default. However, temperature-based equations provide poor estimates of ET_{ref} because they do not account for net radiation or sunshine percentage, vapor pressure deficit, or wind speed, which can play important roles when calculating ET_{ref}, especially under humid/sub-humid regions where the variations in ET_{ref} are more often due to variations in these factors than to variations in temperature. Similarly, the radiation-based equations, including the Priestley-Taylor model, do not account for the impact of the aerodynamic term on ET_{ref}, which can impede the performance of these models in windy and rapidly-changing vapor pressure deficit conditions. These notions can have serious consequences for the way in which ET_{ref} is calculated in climate change models because it has been shown by others and our study that increase in air temperature dos not necessarily result in increasing ET_{ref} rates. The trend and magnitude of ET_{ref} is not a function of temperature, radiation, or any other meteorological parameter alone. Most datasets that are involved in climate change studies are limited only to observed T_{max}, T_{min}, and precipitation, preventing researchers from utilizing energy balance equations. However, it is well-established that estimating ET_{ref} using temperature-based equations can lead to more errors than estimating it using combination-based equations from predicted primary climatic variables. Further, in trend analysis, single variable equations for ET_{ref} inherently pass on the trend of the original variable which can be misleading if several other variables are responsible for changes in ET_{ref}. Here we integrated previously developed practical and robust procedures to estimate necessary climate variables (R_s, R_n, u_2, and VPD) only from observed T_{max} and T_{min}, to be used in the Penman–Monteith-type combination-based energy balance equations to predict ET_o and ET_r, which provides more robust assessments of integrated effect of change in meteorological parameters on atmospheric evaporative demand. Thus, it is suggested that effort to be made to utilize combination-based energy balance equations in climate change studies to estimate ET_{ref} to more accurately assess the effect of change in meteorological variables on evapotranspiration and water resources.

References

Balling Jr., R.C., Idso, S.B., 1990. Effects of greenhouse warming on maximum summer temperatures. Agr. Forest Meteorol. 82, 293–299.

Blaney, H.F., Criddle, W.D., 1950. Determining Water Requirements in Irrigated Areas from Climatological and Irrigation Data. Soil Conservation Service Technical Paper 96. Soil Conservation Service, US Dept. of Agriculture: Washington, DC.

Brutsaert, W., Parlange, M.B., 1998. Hydrologic cycle explains the evaporation paradox. Nature 396, 30.

Burn, D.H., Hesch, N.M., 2007. Trends in evaporation for the Canadian Prairies. J. Hydrol. 336, 61–73.

Chattopadhyay, N., Hulme, M., 1997. Evaporation and potential evapotranspiration in India under conditions of recent and future climate change. Agr. Forest Meteorol. 87, 55–73.

Chen, D., Gao, G., Xu, C.-Y., Guo, J., Ren, G.-Y., 2005. Comparison of the Thornthwaite method and pan data with the standard Penman-Monteith estimates of reference evapotranspiration in China. Clim. Res. 28, 123–132.

Chen, S., Iu, Y., Thomas, A., 2006. Climatic change on the Tibetan Plateau: potential evapotranspiration trend from 1961–2006. Clim. Change 76, 291–319.

Cohen, S., Ianetz, A., Stanhill, G., 2002. Evaporative climate changes at Bet Dagan, Israel, 1964–1998. Agr. Forest Meteorol. 111, 83–91.

Cong, Z.T., Yang, D.W., 2009. Does evaporation paradox exist in China? Hydrol. Earth Syst. Sci. 13, 357–366.

Curtis, D.C., Eagleson, P.S., 1982. Constrained Stochastic Climate Simulation. Tech. Rep. 274, Mass. Inst. of Technol., Dep. of Civ. and Environ. Eng., Ralph M. Parsons Lab., Cambridge, Mass.

Dai, A., Fung, I.Y., DelGenio, A.D., 1997. Surface observed global land precipitation variations during 1900–88. J. Clim. 10, 2943–2962. doi:10.1175/1520-0442(1997)010<2943:SOGLPV>2.0.CO;2.

Doorenbos, J., Pruitt, W.O., 1977. Guidelines for Prediction of Crop Water Requirements. FAO Irrig. and Drain. Paper No. 24 (revised), Rome, Italy. 144 pp.

Duffie, J.A., Beckman, W.A., 1980. Solar Engineering of Thermal Processes. J. Willey, New York, pp. 109.

Gao, G., Chen, D., Ren, G.Y., Chen, Y., Liao, Y.M., 2006. Spatial and temporal variations and controlling factors of potential evapotranspiration in China: 1956–2000. J. Geogr. Sci. 16 (1), 3–12.

Gao, G., Chen, D., Xu, C.-Y., Simelton, E., 2007. Trend of estimated actual evapotranspiration over China during 1960–2002. J. Geophys. Res. 112, D11120. doi:10.1029/2006JD008010.

Gedney, N., Cox, P.M., Betts, R.A., Boucher, O., Huntingford, C., Stotts, P.A., 2006. Detection of a direct carbon dioxide effect in continental river runoff records. Nature 439, 835–838. doi:10.1038/nature04504.

Golubev, V.S., Lawrimore, J.H., Groisman, P.Y., Speranskaya, N.A., Zhuravin, S.A., Menne, M.J., Peterson, T.C., Malone, R.W., 2001. Evaporation changes over the contiguous United States and the former USSR: a reassessment. Geophys. Res. Lett. 28, 2665–2668.

Groisman, P.Y., Knight, R.W., Karl, T.R., Easterling, D.R., Sun, B., Lawrimore, J.H., 2004. Contemporary changes of the hydrological cycle over the contiguous United States: trends derived from in situ observations. J. Hydrometeorol. 5, 64–85.

Grundstein, A., 2009. Evaluation of climate change over the continental United States using a moisture index. Climatic Change 93 (1–2), 103–115.

Gupta, R.S., 2008. Hydrology and Hydraulic Systems, third ed. Waveland Press, Inc., Prospect Heights, Illinois, USA, pp. 388.

Hamelet, A.F., Lettenmaier, D.P., 1999. Columbia River stream-flow forecasting based on ENSO and PDO climate signals. J. Water Resour. Plann. Manage. 125, 333–341.

Hamon, W.R., 1961. Estimating potential evapotranspiration. J. Hydraul. Div. Proc. Am. Soc. Civil Eng. 87, 107–120.

Hargreaves, G.H., Samani, Z.A., 1982. Estimating potential evapotranspiration. J. Irrig. Drain. Eng. 108 (3), 225–230.

Hargreaves, G.H., Samani, Z.A., 1985. Reference crop evapotranspiration from temperature. Appl. Eng. Agric. 1 (2), 96–99.

Hobbins, M.T., Ramirez, J.A., Brown, T.C., 2004. Trends in pan evaporation and actual evapotranspiration across conterminous US: paradoxial or complementary? Geophys. Res. Lett. 31, L13503. doi:10.1029/2004GL019846.

Houghton, J.T., Ding, Y., Griggs, D.J., Nouger, M., van der Linden, P.J., Dai, X., Maskell, K., Johnson, C.A., 2001. Climate Change 2001: The Scientific Basis. Intergovernmental Panel on Climate Change. Cambridge Univ. Press, Cambridge, U.K., 822 pp.

Hubbard, K.G., 1992. Climatic factors that limit daily evapotranspiration in sorghum. Clim. Res. 2, 73–80.

Hubbard, K.G., Guttman, N.B., You, J., Chen, Z., 2007. An improved QC process for temperature in the daily cooperative weather observations. J. Atmos. Oceanic Technol. 24, 206–213.

Hulme, M., Osborn, T.J., Johns, T.C., 1998. Precipitation sensitivity to global warming: comparison of observations with HadCM2 simulations. Geophys. Res. Lett. 25, 3379–3382. doi:10.1029/98GL02562.

Huntington, T.G., 2006. Evidence for intensification of the global water cycle: review and synthesis. J. Hydrol. 319, 83–95.

IPCC, 1996. Climate Change 1995: Impacts, Adaptation and Mitigation of Climate Change: Scientific-Technical Analyses. Contribution of Working Group II to the Second Assessment Report of the Intergovernmental Panel on Climate Change. In: Watson, R.T., Zinyowera, M.C., Moss, R.H., Dokken, D.J. (Eds.), Cambridge Univ. Press, Cambridge Univ. Press, Cambridge, UK.

IPCC, 2007. Summary for policymakers. In: Solomon, S. et al. (Eds.), Climate Change 2007: Impacts, Adaptation and Vulnerability. Contribution of Working Group II to the Fourth Assessment Report of the Intergovernmental Panel on Climate Change. Cambridge Univ. Press, Cambridge, UK.

Irmak, S., Payero, J.O., Martin, D.L., Irmak, A., Howell, T.A., 2006. Sensitivity analyses and sensitivity coefficients of the standardized ASCE-Penman-Monteith equation to climate variables. J. Irrig. Drain. Eng. 132 (6), 564–578.

Irmak, S., Irmak, A., Howell, T.A., Martin, D.L., Payero, J.O., Copeland, K.S., 2008. Variability analyses of alfalfa-reference to grass-reference evapotranspiration ratios in growing and dormant seasons. J. Irrig. Drain. Eng. 134 (2), 147–159.

Irmak, S., 2010. Nebraska water and energy flux measurement, modeling, and research network (NEBFLUX). Trans. ASABE 53 (4), 1097–1115.

Irmak, S., Mutiibwa, D., 2010. On the dynamics of canopy resistance: generalized-linear estimation and its relationships with primary micrometeorological variables. Water Resour. Res. 46 (1–20), W08526. doi:10.1029/2009WR008484.

Irmak, S., Mutiibwa, D., Payero, J.O., 2010. Net radiation dynamics: performance of 20 daily net radiation models as related to model structure and intricacy in two climates. Trans. ASABE 53 (4), 1059–1076.

Ivanov, V.Y., Bras, R.L., Curtis, D.C., 2007. A weather generator for hydrological, ecological, and agricultural applications. Water Resour. Res. 43, W10406.

Jensen, M.E., Haise, H.R., 1963. Estimating evapotranspiration from solar radiation. J. Irrig. Drain. Eng. 89 (IR4), 15–41.

Kahler, D.M., Brusaert, W., 2006. Complementary relationship between daily evaporation in the environment and pan evaporation. Water Resour. Res. 42, W05413.

Karl, T.R., Easterling, D.R., Quayle, R.G., 1996. Indices of climate change for the United States. Bull. Am. Meteor. Soc. 77, 279–292.

Karl, T.R., Knight, R.W., 1998. Secular trends of precipitation amount, frequency, and intensity in the United States. Bull. Am. Meteor. Soc. 79, 231–241.

Kunkel, K.E., Andsager, K., Easterling, D.R., 1999. Long-term trends in extreme precipitation events over the conterminous United States and Canada. J. Climate 12, 2515–2527.

Lawrimore, J.H., Peterson, T.C., 2000. Pan evaporation trends in dry and humid regions of the United States. J. Hydrometeorol. 1, 543–546.

Lettenmaier, D., Wood, E.F., Wallis, J.R., 1994. Hydro-climatological trends in the continental United States: 1948–88. J. Climate 7, 586–607.

Linacre, E.T., 1977. A simple formula for estimating evaporation rates in various climates, using temperature data alone. Agric. Meteorol. 18 (6), 409–424.

Lins, H.F., Michaels, P.J., 1994. Increasing US streamflow linked to greenhouse forcing, EOS. Trans. Am. Geophys. Union 75, 284–285.

Liu, B.H., Xu, M., Henderson, M., Gong, W.G., 2004. A spatial analysis of pan evaporation trends in China, 1955–2000. J. Geophys. Res. 109, D15102, doi:2029/2004JD004511.

Liu, C.M., Zheng, Y., 2004. Changes of pan evaporation in the recent 40 years in the Yellow River Basin. Water Int. 29, 510–516.

Makkink, G.F., 1957. Testing the Penman formula by means of lysimeters. J. Inst. Water Eng. 11 (3), 277–288.

McCabe, G.J., Wolock, D.M., 2002. Trends and temperature sensitivity of moisture conditions in the conterminous United States. Climate Res. 20, 19–29.

Monteith, J.L., 1965. Evaporation and the environment. In: The State and Movement of Water in Living Organisms, XIXth Symposium. Cambridge Univ. Press, Swansea, Wales. Cambridge, UK. pp. 205–234.

Moonen, A.C., Ercoli, L., Mariotti, M., Masoni, A., 2002. Climate change in Italy indicated by agrometeorological indices over 122 years. Agr. Forest Meteorol. 111, 13–27.

Moot, D.J., Henderson, A.L., Porter, J.R., Semenov, M.A., 1996. Temperature, CO_2 and the growth and development of wheat: changes in the mean and variability of growing conditions. Clim. Change 33, 351–368.

Murray, F.W., 1967. On the computation of saturated vapor pressure. J. Appl. Meteorol. 6, 203–204.

Neal, E.G., Walter, M.T., Coffeen, C., 2002. Linking the Pacific decadal oscillation to seasonal stream discharge patterns in southeast Alaska. J. Hydrol. 263, 188–197.

Ohmura, A., Wild, M., 2002. Is the hydrological cycle accelerating? Science 298, 1345–1346.

Penman, H.L., 1948. Natural evaporation from open water, bare soil and grass. Proc. Roy. Soc. London A193, 120–146.

Penman, H.L., 1963. Vegetation and Hydrology. Tech. Comm. No. 53, Commonwealth Bureau of Soils, Harpenden, England. 125 p.

Peterson, T.C., Golubev, V.C., Groisman, P.Y., 1995. Evaporation losing its strength. Nature 377, 687–688.

Priestley, C.H.B., Taylor, R.J., 1972. On the assessment of surface heat flux and evaporation using large-scale parameters. Monthly Weather Rev. 100 (2), 81–92.

Qian, T., Dai, A., Trenberth, K.E., 2007. Hydroclimatic trends in the Mississippi River Basin from 1948 to 2004. J. Climate 20, 4599–4614.

Rayner, D.P., 2007. Wind run changes: the dominant factor affecting pan evaporation trends in Australia. J. Climate 20, 3379–3394.

Ren, G.Y., Guo, J., 2006. Change in pan evaporation and the influential factors over China: 1956–2000 (in Chinese with English abstract). J. Nat. Resour. 21 (1), 31–44.

Roderick, M.L., Farquhar, G.D., 2002. The cause of decreased pan evaporation over the past 50 years. Science 298, 1410–1411.

Roderick, M.L., Farquhar, G.D., 2004. Changes in Australian pan evaporation from 1970 to 2002. Int. J. Climatol. 24, 1077–1090.

Roderick, M.L., Rotstayn, L.D., Farquhar, G.D., Hobbins, M.T., 2007. On the attribution of changing pan evaporation. Geophys. Res. Lett. 34, L17403, doi:17410.11029/12007GL031166.

Samani, Z., 2000. Estimating solar radiation and evapotranspiration using minimum climatological data. J. Irrig. Drain. Eng. 126 (4), 265–267.

Thomas, A., 2000. Spatial and temporal characteristics of potential evapotranspiration trends over China. Int. J. Climatol. 20, 381–396.

Thornthwaite, C.W., 1948. An approach toward a rational classification of climate. Geogr. Rev. 38, 55–94.

Trenberth, K.E.L., Smith, T., Qian, A. Dai, Fasullo, J., 2007. Estimate of the global water budget and its annual cycle using observational and model data. J. Hydrometeorol. 8, 758–769.

Turc, L., 1961. Evaluation des besoins en eau d'irrigation, evapotranspiration potentielle, formule climatique simplifiee et mise a jour. Ann. Agron. 12 (1), 13–49.

Wang, Y., Jiang, T., Bothe, O., Fraedrich, K., 2007. Changes of pan evaporation and reference evaporation in the Yangtze River basin. Theor. Appl. Climatol. 90, 13–23.

Xu, C.Y., Gong, L.B., Jiang, T., Chen, D.L., Singh, V.P., 2006. Analysis of spatial distribution and temporal trend of reference evapotranspiration and pan evaporation in Changjing (Yangtze River) catchment. J. Hydrol. 327, 81–93.

Yin, Y., Wu, S., Chen, G., Dai, E., 2010. Attribution analyses of potential evapotranspiration changes in China. Theor. Appl. Climatol. 101, 19–28.

Zhang, Y., Liu, C., Tang, Y., Yang, Y., 2007. Trends in pan evaporation and reference and actual evapotranspiration across the Tibetan Plateau. J. Geophys. Res. 112, D12110. doi:10.1029/2006JD008161.

Zheng, H., Liu, X., Liu, C., Dai, X., 2009. Assessing contributions to panevaporation trends in Haihe River Basin, China. J. Geophys. Res. Lett. 114, D24105. doi:10.1029/2009JD012203.